Leachate Pressure Effect on a System Reliability–Based Design of Reinforced Soil Walls for a Vertical Expansion of MSW Landfills

Shilpi Mahapatra[1]; B. Munwar Basha, M.ASCE[2]; and Bappaditya Manna, M.ASCE[3]

Abstract: The issue of vertical capacity expansion of municipal solid waste (MSW) landfills with reinforced soil walls (RSWs) is addressed in the present investigation. The influence of different conditions of leachate levels in MSW landfills is a major cause of translational failures. Poor hydraulic conductivity, clogging of drainage because of fines, and freezing of drainage in landfills are the crucial factors of the buildup of leachate pressure. Heterogeneity and different fill ages in MSW landfills gradually change the inherent properties of landfills. The assumption-independent component failures of sliding, eccentricity, bearing capacity, tension, and pullout modes in predicting the series system reliability index of RSWs against translational failure under six leachate level conditions may produce large errors because component failures are usually dependent on one another. Therefore, the present paper demonstrates the feasibility of considering dependent failure modes to estimate the dimensions of RSWs to maintain the external and internal stability under six different leachate buildup conditions. The variability associated with the cohesion of solid waste, the apparent cohesion between liner components beneath the wedges, the friction angle of MSW, and the interface friction angle beneath the wedges is considered for the estimation of the lower bound of the series system reliability index. The limit equilibrium method is employed to assess the stability of an RSW for an expanded MSW landfill. Further, the design charts for the optimum values of width and height of the RSW are provided for different leachate levels (h_w) under six leachate buildup conditions by targeting various lower bounds of a system reliability index ≥3.0. The design values of the number of reinforcement layers (n) are also provided corresponding to the optimum dimensions of the RSW subjected to different leachate levels. **DOI: 10.1061/IJGNAI.GMENG-7755**.

Author keywords: Leachate levels; Translational failure; Municipal solid waste (MSW); Reinforced soil wall; Reliability; Target reliability index; Vertical expansion.

Introduction

A leachate is any liquid that is squeezed out from the decomposition or compaction of waste. Further, it gets percolated through a landfill by precipitation, irrigation, or recirculation of leachate. An engineered landfill commonly has a collection system for leachate. The leachate collection system (LCS) is designed in such a way that it can collect and remove the leachate from the base of the landfill. Hence, the LCS minimizes the building up of the leachate head. However, leakage of contaminants can occur due to defects in the liner because the driving force may develop due to the leachate head. The performance of the LCS is a crucial factor in the case of an engineered landfill. The clogging of drainage pipes, noncollection of leachate in old landfills, and freezing of drainage in landfills are some factors of concern for the buildup of leachate. Furthermore, low hydraulic conductivity or blocking of the LCS is induced because of leachate constituents (inorganic material, fatty acids, and suspended solids), chemical precipitation, bacterial growth, and accumulation of particulate material. The service life of the LCS also plays a critical role in municipal solid waste (MSW) landfills due to clogging of the drainage pipes. An improper design of the LCS further leads to the mounding of leachate on the bottom liner of the landfill. The buildup of leachate in landfills is the major cause of translational failures because it affects the stability of landfills. It has been observed that the improper management of leachate had caused catastrophic failures in the past.

[1]Formerly, Research Scholar, Dept. of Civil Engineering, IIT Delhi, Delhi 110016, India; currently, Design Engineer-Geotechnical-Bridges & Civils, Ramboll, The Epitome, Building No. 5, Tower-B, Floor-17, DLF Cyber Terrace Phase-III, Gurugram 122002, India. Email: shilpi07.iitd@gmail.com

[2]Associate Professor, Dept. of Civil Engineering, Indian Institute of Technology Hyderabad, 502285 Telangana, India (corresponding author). ORCID: https://orcid.org/0000-0003-1417-3650. Email: basha@ce.iith.ac.in

[3]Professor, Dept. of Civil Engineering, Indian Institute of Technology, Delhi 110016, India. Email: bmanna@civil.iitd.ac.in

Note. This manuscript was submitted on February 20, 2022; approved on October 23, 2022; published online on February 7, 2023. Discussion period open until July 7, 2023; separate discussions must be submitted for individual papers. This paper is part of the ***International Journal of Geomechanics***, © ASCE, ISSN 1532-3641.

Review of the Literature

Failures in the Past due to Excessive Leachate Buildup

A few landfill failures due to excessive leachate buildup are as follows: (1) MSW landfill failure in Istanbul in 1993 (Kocasoy and Curi 1995), (2) slope failure of the Hiriya landfill in 1997 (Isenberg 2003), and (3) the case of the Payatas Landfill in the Philippines in 2000 (Merry et al. 2005). Therefore, leachate pressure in MSW landfills may play a crucial role in landfill slope failures, and it should be given due consideration while designing a landfill. Ling et al. (1998) discussed the settlement of an MSW landfill and further proposed a tool to identify the settlement by using

empirical relationships. It is also reported that utilities may get impaired due to differential settlements in landfills. The factors that affect these settlements are the heterogeneity of waste mass combined with an unsaturated landfill. Koerner and Soong (2002) illustrated the impact of leachate on landfill stability. The increase in leachate head may cause insufficient frictional resistance between the liner and the waste mass. Further, it leads to landfill failure. By means of field and laboratory studies, Rowe and Yu (2010) explained the various factors that can affect the clogging of LCSs in landfills. It is observed that the grain size distribution of drainage material, effect of temperature, and increased leachate flow escalate the rate of clogging of the drainage layer. Jafari et al. (2017) discussed the effect of elevated temperatures on the increase in the volume of leachate in landfills, which leads to the movement of slope, and unusual settlements in landfills. Hence, elevated temperatures can damage the infrastructure of landfills.

Leachate Levels in MSW Landfills

The stability of waste mass is also dependent upon the quantity of leachate generated in a landfill. Improper design of the leachate collection system may cause the failure of landfills. Jang et al. (2002) analyzed leachate levels of up to 30 m in height in the Kimpo Metropolitan Landfill, Seoul, Korea. Young-Soek et al. (2022) reported that the maximum height of the landfill was recorded to be 44.10 m when landfilling was completed in 2000. Leachate levels ranging from 10 to 14 m were observed in a field investigation. It is suggested that the leachate level is directly correlated with the height of a waste fill. Qian and Koerner (2007) performed studies on the failure of eight landfills in 20 years. These failures have happened primarily due to high leachate levels within the solid waste mass. Out of these eight, four were geomembrane- or composite-lined landfills. It is noted that the leachate head should not be more than 300 mm as regulated by the Environmental Protection Agency (EPA) in the USA.

Zhan et al. (2015) observed a leachate mound with a peak height of 15 m in the Qizishan Landfill in Suzhou, China. High leachate mounds have been reported in a significant number of MSW landfills in China. This can be attributed to high organic and water content, poor serviceability and clogging of the drainage system, poor management of surface water, and heavy rainfall greater than 10 cm in humid regions. Gao et al. (2018) studied the slope stability analysis of MSW landfills. It is reported that the leachate level needs to be controlled to ensure landfill stability. Yang et al. (2019) discussed the effect of permeability within the waste mass and the degree of clogging of the drainage layer. They reported that the dissipation of the pore-water pressure (PWP) was slow because of an increase in leachate levels due to clogging in the landfill. Khasawneh and Zhang (2020) investigated the slope failure of the Doña Juana MSW Landfill caused by excessive PWP due to a recirculation of leachate. They performed numerical simulations to analyze the failure mechanism and found the hydraulic fracturing within the waste and the clay liner close to the landfill slope. Yang et al. (2020) discussed the operational safety of landfills for rainfall conditions. They suggested drainage measures near the waste slopes at the downstream, where the perched leachate levels were found to be high. Zhang et al. (2020) studied 62 MSW landfills from 22 different countries to analyze the causes of their instability and found that a high landfill leachate level was the predominant reason in 40.32% of landfills. It is found that high levels of organic waste, high rainfall, accumulation of plastics, and landfill gas cause an increase in leachate levels, further reducing the shear strength of MSW, which, in turn, leads to the instability of landfills.

Stability Analysis of MSW Landfills by the Deterministic Approach

Qian (2008) described the issue of landfill translational failure subject to four leachate buildup cases. A liner with a high interface friction angle and low apparent cohesion decreases the factor of safety (FS) faster than that with a low interface friction angle and high apparent cohesion with the increase in leachate levels. Choudhury and Savoikar (2010) evaluated the seismic stability of typical side-hill-type MSW landfills and reported that the horizontal seismic acceleration coefficient has a significant influence on the factor of safety. Savoikar and Choudhury (2012) introduced equations for minimum and maximum factors of safety against translational failure and for the yield acceleration for landfills under seismic loading both in the horizontal and in the vertical directions by using the pseudodynamic method. Ering and Babu (2016) implemented a constitutive modeling approach for stability and deformation analysis, including the influence of loading, biodegradation, and mechanical degradation of an MSW landfill slope. Annapareddy et al. (2017) observed the susceptibility of seismic damage in low-frequency input motions in a landfill using a modified pseudodynamic method. Sheng et al. (2021) studied the four slope instability modes for a vertical expansion of a landfill under six leachate buildup conditions. They reported that the safety factor of the landfill decreased by 13.2%–15.4% as the height of the leachate level increased from 2 to 20 m.

Reliability-Based Design of MSW Landfills

The design of landfills using the traditional factor of safety does not include the heterogeneity associated with the MSW shear strength properties. Reliability-based design optimization using first-order and second-order reliability methods is required to quantify the uncertainties (Babu and Basha 2008; Raghuram and Basha 2021). Mahapatra et al. (2020) proposed stability analysis using a system reliability–based design of an MSE wall for an MSW landfill under vertical expansion. The optimum height and the reinforcement length of the MSE wall were computed to obtain the targeted system reliability value against sliding, eccentricity, and bearing capacity failures.

Objectives and Scope of the Present Study

The present study uses the analysis proposed by Qian (2008) for examining the translational failure of four seepage cases. Two additional leachate buildup conditions are considered when a reinforced soil wall (RSW) is constructed in front of an MSW landfill for expansion. The expressions for PWPs on a three-part wedge for various seepage conditions are derived and presented. Perhaps this is the first study to investigate the application of series system reliability–based design optimization considering various leachate pressures on the optimum dimensions of an RSW needed for the vertical expansion of an MSW landfill. The present work also demonstrates the feasibility of considering dependent failure modes to estimate the series system reliability index under different leachate buildup conditions for vertically expanded MSW landfills. The objectives of this study are as follows:

1. The dimensions of the RSW are optimized to maintain the targeted value of the lower bound of the system reliability index for vertically expanded MSW landfills under six different leachate buildup conditions.

2. The optimum number of reinforcement layers is provided against the design length of the reinforcement layer to maintain both internal and external stability simultaneously.

Computation of Leachate Pressures for Different Buildup Conditions

The external and internal stability failure modes under six different leachate buildup conditions are shown in Figs. 1(a–f). Furthermore, the forces acting on Wedge1, Wedge2, and the RSW are shown in Figs. 2(a–d).

Case 1: Buildup of Seepage Parallel to the Back Slope and Subgrade

The assumption of Case 1 is that the leachate flows parallelly to the back slope and the subgrade of the landfill. It occurs under the normal operating condition of a landfill, as shown in Fig. 1(a). It simplifies the estimation of the leachate head over the liner, although, practically, the phreatic surfaces are not parallel (McEnroe 1993; Giroud et al. 2000; Qian et al. 2004). According to regulatory requirements in European countries and the USA, the maximum leachate head on a landfill bottom liner should not exceed 300 mm. The resultant pore-water pressures acting on the lateral sides of the Wedge1 (U_{H1}) and Wedge2 (U_{H2}), as shown in Figs. 2(a and b), are given by

$$U_{H1} = U_{H2} = 0.5\gamma_w h_w^2 \cos^2\theta \tag{1}$$

where γ_w = unit weight of water; h_w = depth of leachate as measured vertically from the toe of the back slope; and θ = angle of the landfill cell subgrade with the horizontal. The resultant PWP on the lateral side of the RSW (U_{HB}) is given by

$$U_{HB} = 0.5\gamma_w h_w^2 \cos^2\theta \tag{2}$$

The resultant PWP on the bottom of Wedge1, U_{N1}, is given by

$$U_{N1} = \left[\begin{array}{l} \gamma_w h_{wb}\cos^2\psi\left\{\dfrac{H_1}{\sin\psi} - 0.5\left(h_w\cos\theta - \dfrac{h_{wb}\cos^2\psi}{\cos\theta}\right)\left(\dfrac{1}{\sin(\psi-\theta)}\right) - 0.5\left(\dfrac{h_{wb}\cos\psi}{\tan\psi}\right)\right\} \\ +0.5\gamma_w h_w\cos^2\theta\left(h_w\cos\theta - \dfrac{h_{wb}\cos^2\psi}{\cos\theta}\right)\left(\dfrac{1}{\sin(\psi-\theta)}\right) \end{array}\right] \tag{3}$$

where H_1 = height of the back slope; ψ = angle of the back slope with the horizontal; and h_{wb} = vertical depth of the leachate in the landfill for Cases 1, 3, and 5 [Figs. 1(a, c, and e)] as measured along the back slope. The resultant PWP on the bottom of Wedge2 (U_{N2}) is given by

$$U_{N2} = 0.5\gamma_w h_w \cos^2\theta(KI)/\cos\theta \tag{4}$$

when $B < H_1/\tan\psi$

$$\mathrm{KI} = \frac{\left\{H_1 - \left(\dfrac{H_1}{\tan\psi} - B\right)\tan\eta - H_2\right\}}{(\tan\eta - \tan\theta)} \tag{5}$$

when $B \geq H_1/\tan\psi$

$$KI = \frac{\left\{H_1 + \left(B - \dfrac{H_1}{\tan\psi}\right)\tan\theta - H_2 + \left(B - \dfrac{H_1}{\tan\psi}\right)(\tan\eta - \tan\theta)\right\}}{(\tan\eta - \tan\theta)} \tag{6}$$

where B = width of the waste mass at the top of the back slope; η = angle of the front slope with the horizontal; and H_2 = height of the RSW.

Case 2: Buildup of a Seepage Parallel-to-Subgrade

In this case, the flow of the leachate is parallel to the subgrade, and the head of the leachate is more than the established regulatory value of 300 mm. Hence, this case occurs when the rate of inflow becomes more than the maximum design flow capacity of the discharge system [refer to Fig. 1(b)]. It is observed that the phreatic surface continues beyond the plane of failure. The failure surface occurs within the solid waste at the back slope. Here, it should be mentioned that the expressions for the calculation of the resultant PWP on the lateral side of Wedge2, U_{H2} [Eq. (1)], the resultant PWP on the lateral side of the RSW, U_{HB} [Eq. (2)], and the resultant PWP at the bottom of Wedge2, U_{N2} [Eq. (4)], were provided in the previous section. The resultant PWP on the bottom of Wedge1 (U_{N1}) is given by

$$U_{N1} = \frac{0.5\gamma_w h_w^2 \cos^3\theta}{\sin(\psi - \eta)} \tag{7}$$

Case 3: Buildup of Horizontal Seepage along with Seepage Parallel to the Back Slope

In this case, the leachate flow is parallel to the horizontal, and it rises parallel to the back slope, as shown in Fig. 1(c). It may occur for an active landfill if the leachate collection pump loses power or is broken and the front slope has a temporary cover. This causes a rapid buildup of the leachate head in MSW. The increase in the leachate level at the back slope is due to a larger inflow of liquid during periods of heavy rain. The resultant PWP on the lateral sides of Wedge2 and Wedge1 (U_{H2}) can be written as follows:

$$U_{H2} = U_{H1} = 0.5\gamma_w h_w(h_w) = 0.5\gamma_w h_w^2 \tag{8}$$

The resultant PWP on the lateral side of the RSW (U_{HB}) can be written as follows:

when $B < H_1/\tan\psi$

$$U_{HB} = 0.5\gamma_w\left[h_w + \left\{\frac{H_1 - \left(\dfrac{H_1}{\tan\psi} - B\right)\tan\eta - H_2}{(\tan\eta - \tan\theta)}\right\}\tan\theta\right]^2 \tag{9}$$

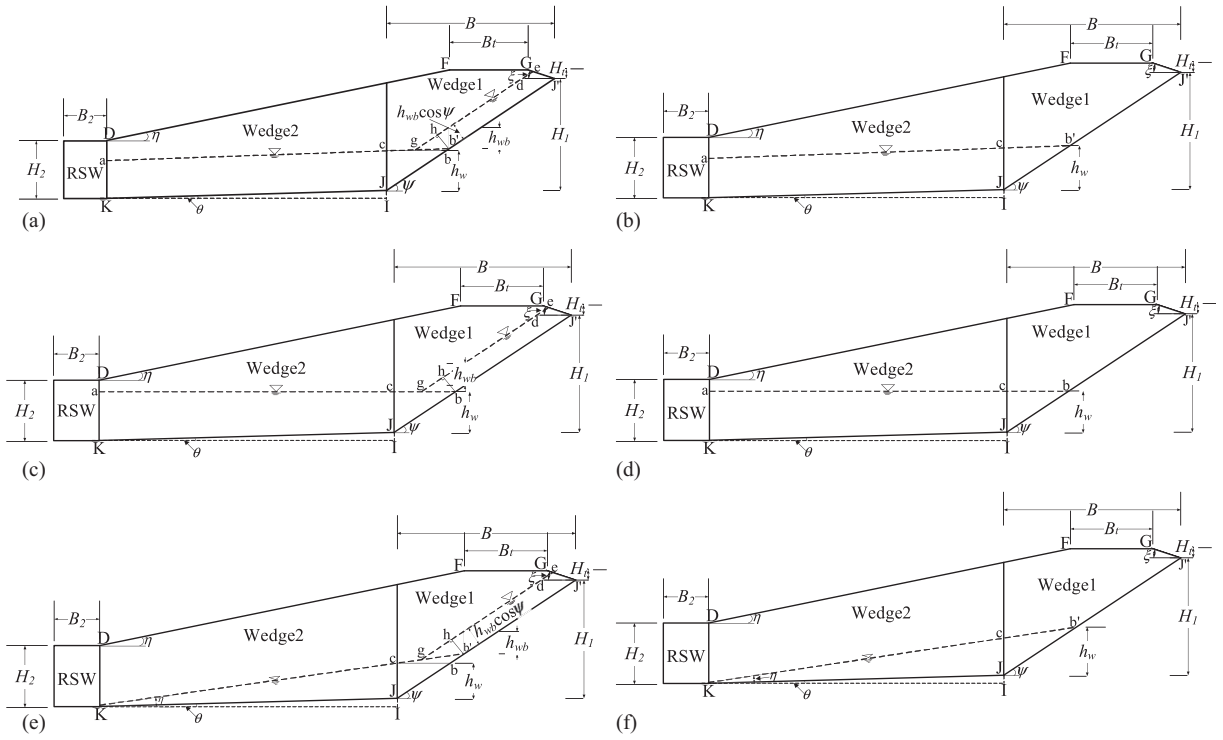

Fig. 1. Six cases of leachate buildup conditions in MSW landfills: (a) parallel-to-subgrade and back slope seepage buildup (Case 1); (b) parallel-to-subgrade seepage buildup (Case 2); (c) parallel-to-horizontal and back slope seepage buildup (Case 3); (d) horizontal seepage buildup (Case 4); (e) parallel-to-front slope of landfill and back slope seepage buildup (Case 5); and (f) parallel-to-front slope of landfill seepage buildup (Case 6).

when $B \geq H_1/\tan\psi$

$$U_{HB} = 0.5\gamma_w \left[h_w + \left\{ \frac{H_1 + \left(B - \frac{H_1}{\tan\psi}\right)\tan\theta - H_2 + \left(B - \frac{H_1}{\tan\psi}\right)(\tan\eta - \tan\theta)}{(\tan\eta - \tan\theta)} \right\} \tan\theta \right]^2 \tag{10}$$

The resultant PWP at the base of Wedge1 (U_{N1}) is depicted as

$$U_{N1} = \left(\frac{0.5\gamma_w h_w^2}{\sin\psi} + \gamma_w h_{wb} \frac{(H - h_w)\cos\psi}{\tan\psi} \right) \tag{11}$$

The resultant PWP on the bottom of Wedge2 (U_{N2})

when $B < H_1/\tan\psi$

$$U_{N2} = \left[\gamma_w \left[h_w + 0.5 \left(\frac{\left\{ H_1 - \left(\frac{H_1}{\tan\psi} - B \right)\tan\eta - H_2 \right\}}{(\tan\eta - \tan\theta)} \right) \tan\theta \right] \frac{\left\{ H_1 - \left(\frac{H_1}{\tan\psi} - B \right)\tan\eta - H_2 \right\}}{(\tan\eta - \tan\theta)} \right] \frac{1}{\cos\theta} \tag{12}$$

when $B \geq H_1/\tan\psi$

$$U_{N2} = \left[\gamma_w \left[h_w + 0.5 \left(\frac{\left\{ H_1 + \left(B - \frac{H_1}{\tan\psi}\right)\tan\theta - H_2 + \left(B - \frac{H_1}{\tan\psi}\right)(\tan\eta - \tan\theta) \right\}}{(\tan\eta - \tan\theta)} \right) \tan\theta \right] \left\{ \frac{H_1 + \left(B - \frac{H_1}{\tan\psi}\right)\tan\theta - H_2 + \left(B - \frac{H_1}{\tan\psi}\right)(\tan\eta - \tan\theta)}{(\tan\eta - \tan\theta)} \right\} \frac{1}{\cos\theta} \right] \tag{13}$$

Case 4: Horizontal Seepage Buildup

The leachate level is considered parallel to horizontal, and there is no leachate buildup at the back slope of the landfill, as illustrated in Fig. 1(d). The buildup occurs for closed or partially closed landfills in case of shutdown problems or power loss of leachate collection and removal pumps. Pump shutdown or clogging of the leachate collection system in a closed landfill causes a high accumulation of leachate at the bottom. Old landfills that might not have such systems are also susceptible to this condition. The expressions for the resultant PWP on the lateral side of Wedge1 (U_{H1}) and Wedge2 (U_{H2}) [Eq. (8)], the resultant PWP on the lateral side of the RSW (U_{HB}) [Eqs. (9) and (10)], and the resultant PWP at the bottom of Wedge2, U_{N2} [Eqs. (12) and (13)], were derived in previous sections. The resultant PWP on the bottom of Wedge1 (U_{N1}) can be obtained by merging $h_{wb} = 0$ into Eq. (11) as

$$U_{N1} = 0.5\gamma_w \frac{h_w^2}{\sin\psi} \tag{14}$$

Case 5: Parallel-to-Front Slope of Landfill and Back Slope Seepage Buildup

The leachate flow is considered parallel to the front slope and back slope of the landfill, as shown in Fig. 1(e). It occurs in an MSW landfill where an RSW is constructed for vertical expansion with a well-functioning leachate collection system. The resultant pore-water pressures acting on the lateral sides of the Wedge1 (U_{H1}) and Wedge2 (U_{H2}), as shown in Figs. 2(a and b), are given by

$$U_{H2} = U_{H1} = 0.5\gamma_w h_w^2 \cos^2\eta \tag{15}$$

The resultant PWP on the bottom of Wedge1 (U_{N1}) can be written as follows:

$$U_{N1} = \left[\begin{array}{l} \gamma_w h_{wb}\cos^2\psi \left\{\begin{array}{l} \dfrac{H_1}{\sin\psi} - 0.5\left(h_w\cos\eta - \dfrac{h_{wb}\cos^2\psi}{\cos\eta}\right)\left(\dfrac{1}{\sin(\psi-\eta)}\right) \\ -0.5\left(\dfrac{h_{wb}\cos\psi}{\tan\psi}\right) \end{array}\right\} \\ +0.5\gamma_w h_w\cos^2\eta\left(h_w\cos\eta - \dfrac{h_{wb}\cos^2\psi}{\cos\eta}\right)\left(\dfrac{1}{\sin(\psi-\eta)}\right) \end{array}\right] \tag{16}$$

The resultant PWP on the bottom of Wedge2 ($U_{N2)}$ can be written as follows when $B < H_1/\tan\psi$

$$U_{N2} = 0.5\gamma_w h_w\cos^2\eta\left[\frac{\left\{H_1 - \left(\dfrac{H_1}{\tan\psi} - B\right)\tan\eta - H_2\right\}}{\cos\theta(\tan\eta - \tan\theta)}\right] \tag{17}$$

when $B \geq H_1/\tan\psi$

$$U_{N2} = 0.5\gamma_w h_w\cos^2\eta\left[\frac{\left\{H_1 + \left(B - \dfrac{H_1}{\tan\psi}\right)\tan\theta - H_2 + \left(B - \dfrac{H_1}{\tan\psi}\right)(\tan\eta - \tan\theta)\right\}}{\cos\theta(\tan\eta - \tan\theta)}\right] \tag{18}$$

Case 6: Parallel-to-Front Slope of Landfill Seepage Buildup

In this case, the flow of leachate is parallel to the front slope of the landfill [refer to Fig. 1(f)]. It occurs in a vertically expanded MSW landfill where the design flow capacity of the collection system is inadequate to remove excess leachate accumulation. The expressions for the resultant PWP on the lateral side of Wedge2 (U_H) [Eq. (15)] and the resultant PWP on the bottom of Wedge2 (U_{N2}) [Eqs. (17) and (18)] were discussed in previous sections. The resultant PWP on the bottom of Wedge1 (U_{N1}) can be written as follows:

$$U_{N1} = \frac{0.5\gamma_w h_w^2\cos^3\eta}{\sin(\psi-\eta)} \tag{19}$$

The detailed steps for the derivation of expressions to calculate the resultant PWPs acting on the bottom of Wedge1 (U_{N1}) for Cases 1–3 and Cases 5 and 6 and the resultant PWP acting on the bottom of Wedge2 (U_{N2}) for Case 3 are presented in the Supplemental Materials.

External Stability of an RSW under Leachate Pressure

The limit equilibrium method is adopted to analyze the stability of an RSW under different leachate buildup conditions (Basha and Basudhar 2010).

Factor of Safety against Sliding Failure Mode

Considering the vertical equilibrium of forces for Wedge1 ($\Sigma F_Y = 0$), as shown in Fig. 2(a), gives

$$W_1 = F_1\sin\psi + N_1\cos\psi + E_{V21} + U_{N1}\cos\psi \tag{20}$$

$$F_1 = N_1 \frac{\tan \delta_1}{FS_1} + \frac{C_1}{FS_1} \tag{21}$$

$$E_{V21} = \frac{C_{sw}}{FS_V} + E_{H21} \frac{\tan \phi_{sw}}{FS_V} \tag{22}$$

where W_1 = weight of Wedge1; F_1 = frictional force on the bottom of Wedge1; N_1 = normal force on the bottom of Wedge1; E_{V21} = frictional force acting on the side of Wedge1; δ_1 = minimum interface friction angle of the liner components underneath Wedge1; FS_1 = factor of safety for Wedge1 of the landfill; C_1 = apparent cohesive force between the liner components underneath Wedge1; C_{SW} = apparent cohesive force of the waste mass; FS_V = factor of safety at the interface between Wedge1 and Wedge2; E_{H21} = normal force acting on Wedge1 from Wedge2; and ϕ_{sw} = angle of the internal friction of the waste mass. The following two assumptions are used in the derivation:

$$m_{sw} = \frac{\tan \phi_{sw}}{FS_V} \tag{23}$$

$$n_{sw} = \frac{C_{sw}}{FS_V} \tag{24}$$

Merging Eqs. (23) and (24) into Eq. (22), we get

$$E_{V21} = n_{sw} + E_{H21} m_{sw} \tag{25}$$

Merging Eqs. (21) and (22) into Eq. (20) gives

$$W_1 = N_1 \left(\cos \psi + \tan \delta_1 \frac{\sin \psi}{FS_1} \right) + E_{H21} m_{sw} + n_{sw} + C_1 \frac{\sin \psi}{FS_1} + U_{N1} \cos \psi \tag{26}$$

Considering the equilibrium of forces in the horizontal direction ($\Sigma F_X = 0$) gives

$$U_{H1} + F_1 \cos \psi + E_{H21} = N_1 \sin \psi + U_{N1} \sin \psi \tag{27}$$

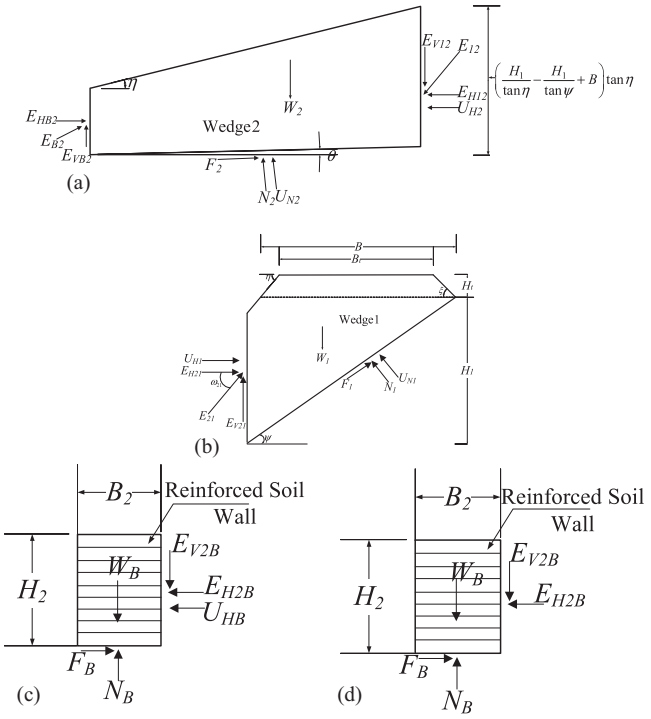

Fig. 2. Free body diagrams: (a) passive wedge of an MSW landfill; (b) active wedge of an MSW; (c) RSW for Cases 1–4 of leachate buildup conditions; and (d) RSW for Cases 5 and 6 of leachate buildup conditions.

Merging Eq. (21) into Eq. (27) and rearranging for N_1 give

$$N_1 = \frac{U_{H1} + E_{H21} - U_{N1} \sin \psi + C_1 \frac{\cos \psi}{FS_1}}{\sin \psi - \cos \psi \frac{\tan \delta_1}{FS_1}} \tag{28}$$

Merging Eq. (28) into Eq. (26) and rearranging for E_{H21} give

$$E_{H21} = \left\{ \frac{(W_1 - n_{sw}) \left(\sin \psi - \cos \psi \frac{\tan \delta_1}{FS_1} \right) - \frac{C_1}{FS_1} + \left(U_{N1} \frac{\tan \delta_1}{FS_1} \right) - U_{H1} \left(\cos \psi + \frac{\sin \psi \tan \delta_1}{FS_1} \right)}{\cos \psi + \sin \psi \frac{\tan \delta_1}{FS_1} + m_{sw} \sin \psi - \cos \psi \tan \delta_1 \frac{m_{sw}}{FS_1}} \right\} \tag{29}$$

Refer to Supplemental Materials for detailed calculations of E_{H21}. Considering the vertical equilibrium of forces for Wedge2 ($\sum F_Y = 0$), as shown in Fig. 2(b), gives

$$W_2 + E_{V12} = N_2 \cos \theta + F_2 \sin \theta + E_{VB2} + U_{N2} \cos \theta \tag{30}$$

The frictional force on the bottom of Wedge2 (F_2) is shown as follows:

$$F_2 = \frac{C_2}{FS_2} + N_2 \frac{\tan \delta_2}{FS_2} \tag{31}$$

The frictional force on the side of Wedge2 (E_{V12}) is written as follows:

$$E_{V12} = \frac{C_{SW}}{FS_V} + E_{H21} \frac{\tan \phi_{sw}}{FS_V} \tag{32}$$

The frictional force on the side of Wedge2 next to the block wedge (E_{VB2}) is given by

$$E_{VB2} = \frac{C_{2B}}{FS_V} + E_{HB2} \left(\frac{\tan \delta_{2B}}{FS_V} \right) \tag{33}$$

where W_2 = weight of Wedge2; N_2 = normal force at the base of Wedge2; C_2 = apparent cohesive force between the liner components underneath Wedge2; FS_2 = factor of safety for Wedge2 of a

landfill; δ_2 = minimum angle of the interface friction of the liner components underneath Wedge2; E_{H12} = normal force acting on Wedge2 from Wedge1; C_{2B} = apparent cohesive force between the RSW and Wedge2; E_{HB2} = normal force acting on Wedge2 from the block wedge; and δ_{2B} = minimum angle of the interface friction between Wedge2 of the landfill and the RSW. It is assumed that

$$n_{2B} = \frac{C_{2B}}{FS_V} \tag{34}$$

Merging Eqs. (23) and (24) into Eq. (32) gives

$$E_{V12} = n_{sw} + E_{H12} m_{sw} \tag{35}$$

Merging Eq. (34) into Eq. (33) gives

$$E_{VB2} = n_{2B} + E_{HB2}\left(\frac{\tan\delta_{2B}}{FS_V}\right) \tag{36}$$

Merging Eqs. (31), (35), and (36) into Eq. (30) gives

$$W_2 + E_{H12} m_{sw} + n_{sw} = \left\{ \begin{array}{l} N_2\left(\cos\theta + \tan\delta_2 \dfrac{\sin\theta}{FS_2}\right) + U_{N2}\cos\theta \\ + C_2 \dfrac{\sin\theta}{FS_2} + E_{HB2}\left(\dfrac{tan\,\delta_{2B}}{FS_V}\right) + n_{2B} \end{array} \right\} \tag{37}$$

Horizontal equilibrium of forces ($\sum F_X = 0$) gives

$$E_{H12} + N_2 \sin\theta + U_{N2}\sin\theta + U_{H2} = F_2\cos\theta + E_{HB2} \tag{38}$$

Merging Eq. (31) into Eq. (38) and rearranging for N_P give

$$N_2 = \frac{E_{HB2} - E_{H12} + C_2\cos\theta/FS_2 - U_{N2}\sin\theta - U_{H2}}{\sin\theta - \cos\theta\tan\delta_2/FS_2} \tag{39}$$

Merging Eq. (39) into Eq. (37) gives (refer to Supplemental Materials for more information)

$$\begin{aligned} &\left[(W_2 + n_{sw} - n_{2B})\left(\sin\theta - \cos\theta\frac{\tan\delta_2}{FS_2}\right) - \frac{C_2}{FS_2} + U_{N2}\frac{\tan\delta_2}{FS_2} + U_{H2}\left(\cos\theta + \tan\delta_2\frac{\sin\theta}{FS_2}\right)\right] \\ &= \left[\begin{array}{l} E_{HB2}\left(\cos\theta + \tan\delta_2\dfrac{\sin\theta}{FS_2} + \left(\dfrac{\tan\delta_{2B}}{FS_V}\right)\left(\sin\theta - \cos\theta\dfrac{\tan\delta_2}{FS_2}\right)\right) \\ -E_{H12}\left(\cos\theta + \tan\delta_2\dfrac{\sin\theta}{FS_2} + m_{sw}\left(\sin\theta - \cos\theta\dfrac{\tan\delta_2}{FS_2}\right)\right) \end{array}\right] \end{aligned} \tag{40}$$

Considering the vertical equilibrium of forces for the RSW ($\sum F_Y = 0$) for Cases 1–4 of leachate buildup conditions, as shown in Fig. 2(c), gives

$$W_B + E_{V2B} = N_B \tag{41}$$

$$E_{V2B} = \frac{C_{2B}}{FS_V} + E_{H2B}\frac{\tan\delta_{2B}}{FS_V} \tag{42}$$

$$E_{V2B} = n_{2B} + E_{H2B}\frac{\tan\delta_{2B}}{FS_V} \tag{43}$$

where W_B = weight of the RSW; E_{V2B} = frictional force on the side of the block wedge next to Wedge2; E_{H2B} = normal force acting on the block wedge from Wedge2; and N_B = normal force at the base of the RSW. Merging Eq. (43) into Eq. (41) gives

$$W_B + n_{2B} + E_{H2B}\frac{\tan\delta_{2B}}{FS_V} = N_B \tag{44}$$

Horizontal equilibrium of forces ($\sum F_X = 0$) gives

$$E_{H2B} + U_{HB} = F_B \tag{45}$$

where F_B = frictional force at the base of the RSW is written as follows:

$$F_B = \frac{C_B}{FS_B} + N_B\frac{\tan\delta_b}{FS_B} \tag{46}$$

Merging Eq. (45) into Eq. (46) gives

$$N_B = \frac{E_{H2B} + U_{HB} - C_B/FS_B}{\tan\delta_b/FS_B} \tag{47}$$

where C_B = apparent cohesive force between the liner components underneath the RSW; and δ_b = minimum angle of the interface friction of the liner components underneath the RSW, and FS_B = factor of safety for the RSW. Merging Eq. (47) into Eq. (44) and rearranging for E_{H2B} give (refer to Supplemental Materials for detailed calculations)

$$E_{H2B} = \frac{(W_B + n_{2B})\left(\dfrac{\tan\delta_b}{FS_B}\right) - U_{HB} + \dfrac{C_B}{FS_B}}{1 - \left(\dfrac{\tan\delta_b}{FS_B}\right)\left(\dfrac{\tan\delta_{2B}}{FS_V}\right)} \tag{48}$$

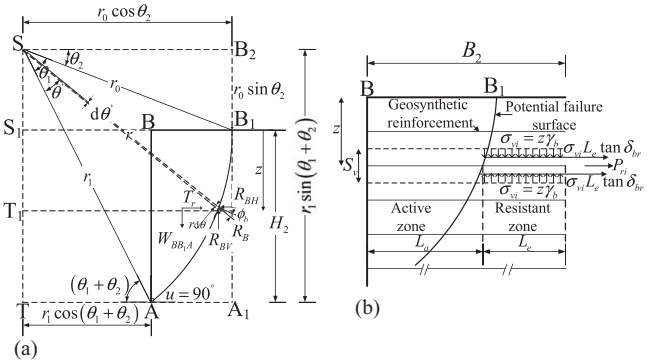

Fig. 3. Internal stability analysis of an RSW: (a) log-spiral failure mechanism of an RSW for a static condition; and (b) illustration of resisting force calculation against pullout failure.

Because $E_{HB2}=E_{H2B}$, $E_{H12}=E_{H21}$, and $FS_V=FS_B=FS_1=FS_2=FS_{sli}$, merging Eqs. (48) and (29) into Eq. (40) gives

$$\left[(W_2+n_{sw}-n_{2B})\left(\sin\theta-\cos\theta\frac{\tan\delta_2}{FS_{sli}}\right)-\frac{C_2}{FS_{sli}}+U_{N2}\frac{\tan\delta_2}{FS_{sli}}+U_{H2}\left(\cos\theta+\tan\delta_2\frac{\sin\theta}{FS_{sli}}\right)\right]$$
$$=\left[\begin{array}{l}\left\{\dfrac{(W_B+n_{2B})\left(\dfrac{\tan\delta_b}{FS_{sli}}\right)-U_{HB}+\dfrac{C_B}{FS_{sli}}}{1-\left(\dfrac{\tan\delta_b}{FS_{sli}}\right)\left(\dfrac{\tan\delta_{2B}}{FS_{sli}}\right)}\right\}\left\{\begin{array}{l}\cos\theta+\tan\delta_2\dfrac{\sin\theta}{FS_{sli}}\\+\left(\dfrac{\tan\delta_{2B}}{FS_{sli}}\right)\left(\sin\theta-\cos\theta\dfrac{\tan\delta_2}{FS_{sli}}\right)\end{array}\right\}\\-\left\{\begin{array}{l}(W_1-n_{sw})\left(\sin\psi-\cos\psi\dfrac{\tan\delta_1}{FS_{sli}}\right)-\dfrac{C_1}{FS_{sli}}\\+\left(U_{N1}\dfrac{\tan\delta_A}{FS_{sli}}\right)-U_{H1}\left(\cos\psi+\dfrac{\sin\psi\tan\delta_1}{FS_{sli}}\right)\\\hline\cos\psi+\sin\psi\dfrac{\tan\delta_1}{FS_{sli}}+m_{sw}\sin\psi-m_{sw}\cos\psi\dfrac{\tan\delta_1}{FS_{sli}}\end{array}\right\}\left\{\begin{array}{l}\cos\theta+\tan\delta_2\dfrac{\sin\theta}{FS_{sli}}\\+m_{sw}\left(\sin\theta-\cos\theta\dfrac{\tan\delta_2}{FS_{sli}}\right)\end{array}\right\}\end{array}\right] \tag{49}$$

The free body diagram of an RSW for Case 5 and Case 6 of leachate buildup conditions is shown in Fig. 2(d). The force equilibrium of an RSW in the vertical direction was discussed previously [refer to Eq. (44)]. Therefore, the horizontal equilibrium of forces ($\sum F_X=0$) gives

$$E_{H2B}=F_B \tag{50}$$

Merging Eq. (46) into Eq. (50) gives

$$N_B=\frac{E_{H2B}-C_B/FS_B}{\tan\delta_B/FS_B} \tag{51}$$

Merging Eq. (51) into Eq. (44) and rearranging for E_{H2B} give (refer to Supplemental Materials for detailed calculations):

$$E_{H2B}=\frac{(W_B+n_{2B})\left(\dfrac{\tan\delta_b}{FS_B}\right)+\dfrac{C_B}{FS_B}}{1-\left(\dfrac{\tan\delta_b}{FS_B}\right)\left(\dfrac{\tan\delta_{2B}}{FS_V}\right)} \tag{52}$$

Because $E_{HB2}=E_{H2B}$, $E_{H12}=E_{H21}$, and $FS_V=FS_B=FS_1=FS_2=FS_{sli}$, merging Eqs. (52) and (29) into Eq. (40) gives

$$\left[(W_2+n_{sw}-n_{2B})\left(\sin\theta-\cos\theta\frac{\tan\delta_2}{FS_{sli}}\right)-\frac{C_2}{FS_{sli}}+U_{N2}\frac{\tan\delta_2}{FS_{sli}}+U_{H2}\left(\cos\theta+\tan\delta_2\frac{\sin\theta}{FS_{sli}}\right)\right]$$
$$=\left[\begin{array}{l}\left\{\dfrac{(W_B+n_{2B})\left(\dfrac{\tan\delta_b}{FS_{sli}}\right)+\dfrac{C_B}{FS_{sli}}}{1-\left(\dfrac{\tan\delta_b}{FS_{sli}}\right)\left(\dfrac{\tan\delta_{2B}}{FS_{sli}}\right)}\right\}\left\{\cos\theta+\tan\delta_2\dfrac{\sin\theta}{FS_{sli}}+\left(\dfrac{\tan\delta_{2B}}{FS_{sli}}\right)\left(\sin\theta-\cos\theta\dfrac{\tan\delta_2}{FS_{sli}}\right)\right\}\\-\left\{\begin{array}{l}(W_1-n_{sw})\left(\sin\psi-\cos\psi\dfrac{\tan\delta_1}{FS_{sli}}\right)-\dfrac{C_1}{FS_{sli}}\\+\left(U_{N1}\dfrac{\tan\delta_1}{FS_{sli}}\right)-U_{H1}\left(\cos\psi+\dfrac{\sin\psi\tan\delta_1}{FS_{sli}}\right)\\\hline\cos\psi+\sin\psi\dfrac{\tan\delta_1}{FS_{sli}}+m_{sw}\sin\psi-m_{sw}\cos\psi\dfrac{\tan\delta_1}{FS_{sli}}\end{array}\right\}\left\{\begin{array}{l}\cos\theta+\tan\delta_1\dfrac{\sin\theta}{FS_{sli}}\\+m_{sw}\left(\sin\theta-\cos\theta\dfrac{\tan\delta_1}{FS_{sli}}\right)\end{array}\right\}\end{array}\right] \tag{53}$$

The probabilistic constraint as the performance function for the sliding failure mode can be written as follows:

$$g_{sli}=FS_{sli}-1\le 0 \tag{54}$$

Factor of Safety against Eccentricity Failure Mode

The factor of safety against eccentricity failure is given by

$$FS_e=\frac{(B_2/6)}{e} \tag{55}$$

where e = eccentricity of the resulting force striking the base of the RSW. The probabilistic constraint as the performance function for the eccentricity failure mode is expressed as follows:

$$g_e = FS_e - 1 \leq 0 \tag{56}$$

Factor of Safety against Bearing Capacity Failure

The factor of safety against bearing capacity failure is the ratio of the ultimate bearing capacity of a foundation of the RSW (q_u) and vertical stress at the base (σ_v), which is shown as follows:

$$FS_b = \frac{q_u}{\sigma_v} \tag{57}$$

where

$$q_u = c_s N_c + qN_q + 0.5\gamma_s(B_2 - 2e)N_\gamma \tag{58}$$

c_s = cohesion of foundation soil; N_c, N_q, and N_γ = bearing capacity factors; and γ_s = unit weight of foundation soil. The vertical stress at the bottom is given by

$$\sigma_v = \frac{\sum V}{B_2 - 2e} \tag{59}$$

The probabilistic constraint as the performance function for the bearing capacity failure mode can be represented as follows:

$$g_b = FS_b - 1 \leq 0 \tag{60}$$

Table 1. Comparison of average factors of safety (FS_{avg}) obtained in the present study for leachate buildup conditions under the static condition with the values obtained by Qian (2008) for all the four cases where h_w varies from 0 to 6 m

Case	h_w (m)	FS_{avg} (Qian 2008)	FS_{avg} (present study)	Percentage difference
Case 1	0	1.440	1.454	−0.97
	1	1.380	1.393	−0.94
	2	1.310	1.331	−1.60
	3	1.250	1.268	−1.44
	4	1.180	1.204	−2.03
	5	1.120	1.140	−1.79
	6	1.050	1.074	−2.29
Case 2	0	1.450	1.454	−0.28
	1	1.420	1.418	0.14
	2	1.390	1.38	0.72
	3	1.350	1.338	0.89
	4	1.310	1.295	1.15
	5	1.270	1.248	1.73
	6	1.220	1.199	1.72
Case 3	0	1.440	1.436	0.28
	1	1.370	1.375	−0.36
	2	1.300	1.312	−0.92
	3	1.240	1.249	−0.73
	4	1.170	1.186	−1.37
	5	1.110	1.121	−0.99
	6	1.040	1.056	−1.54
Case 4	0	1.440	1.436	0.28
	1	1.400	1.400	0.00
	2	1.370	1.362	0.58
	3	1.330	1.321	0.68
	4	1.300	1.277	1.77
	5	1.250	1.231	1.52
	6	1.200	1.183	1.42

Internal Stability of an RSW under Leachate Pressure

The ratio of geosynthetic reinforcement length to the height of an RSW as obtained from an external stability analysis needs to be checked for internal stability against pullout failure and tension failure modes according to FHWA (2001) guidelines.

Force Equilibrium Method to Calculate the Reinforcement Force, T_r

Considering the force equilibrium in the X-direction ($\sum F_X = 0$), as shown in Fig. 3(a), gives

$$T_r = R_{BH} \tag{61}$$

$$R_{BH} = R_B \cos(\theta_1 + \theta_2 - \theta') \tag{62}$$

where

$$R_{BH} = \int_0^{\theta_1} R_B \cos(\theta_1 + \theta_2 - \theta')\, d\theta' = R_B[\sin(\theta_1 + \theta_2) - \sin\theta_2] \tag{63}$$

$$R_B[\sin(\theta_1 + \theta_2) - \sin\theta_2] = T_r \tag{64}$$

where R_B = resultant force along the radial line of the log-spiral; θ_1= subtended angle of the log-spiral wedge SB_1A; θ_2= angle between the horizontal and the initial radius of the log-spiral wedge SB_1; and θ' = angle between the final radius of the log-spiral wedge (SA) and the radial line of the elemental strip. Considering the vertical equilibrium of forces ($\sum F_Y = 0$) gives

$$R_{BV} = W_{BB_1A} \tag{65}$$

$$R_{BV} = R_B \sin(\theta_1 + \theta_2 - \theta') \tag{66}$$

where

$$R_{BV} = \int_0^{\theta_1} R_B \sin(\theta_1 + \theta_2 - \theta')\, d\theta' = R_B[\cos\theta_2 - \cos(\theta_1 + \theta_2)] \tag{67}$$

Table 2. Input parameters considered for the validation of methodology in this study

Input parameters	Values
B (m)	20
H_1 (m)	30
c_1 (kN/m^2)	12.20
c_2 (kN/m^2)	12.20
δ_1 (°)	9
δ_2 (°)	9°
η (°)	14
θ (°)	1.1
ψ (°)	18.43
c_{sw} (kN/m^2)	3
ϕ_{sw} (°)	30
γ_{sw} (kN/m^3)	10.20
γ_w (kN/m^3)	9.81
$(\gamma_{sw})_{sat}$ (kN/m^3)	12.27
h_w (m)	0–0.6
U (°)	0
α (°)	0
h_{wb} (m)	$0.5h_w$ (Cases 1 and 3)
h_{wb} (m)	0 (Cases 2 and 4)

$$R_B[\cos\theta_2 - \cos(\theta_1 + \theta_2)] = W_{BB_1A} \tag{68}$$

where W_{BB_1A} = weight of the log spiral portion BB_1A.

$$\begin{aligned}\text{Weight of } BB_1A = (&\text{Weight of } SB_1A + \text{Weight of SAT}\\ &- \text{Weight of } SS_1BB_1\\ &- \text{Weight of } S_1\text{BAT})\end{aligned} \tag{69}$$

Refer to Supplemental Materials for detailed calculations.

$$W_{BB_1A} = 0.5\gamma_b r_0^2 \left[\begin{array}{l}\left(\dfrac{e^{2\theta_1\tan\phi_b}-1}{2\tan\phi_b}\right) + \dfrac{e^{2\theta_1\tan\phi_b}\sin 2(\theta_1+\theta_2)}{2}\\ -\dfrac{1}{2}(\sin 2\theta_2) - \dfrac{2H_2 e^{\theta_1\tan\phi_b}\cos(\theta_1+\theta_2)}{r_0}\end{array}\right] \tag{70}$$

where W_{BB_1A} = weight of the log-spiral segment BB_1A; ϕ_b= friction angle of the RSW; and r_0 = initial radius of the log-spiral section BB_1A. The following expression for the reinforcement force (T_r) needed to stabilize the RSW can be obtained by solving Eqs. (64) and (68)

$$T_r = W_{BB_1A}\cot\left(\frac{\theta_1}{2} + \theta_2\right) \tag{71}$$

Factor of Safety against Tension Failure

The large external load on the reinforcement layer leads to excessive deformation and collapse of the RSW. Therefore, the design strength of the reinforcement in tension (T_D) should be adequate to resist the maximum possible load. The factor of safety against tension failure is shown as follows:

$$FS_t = \frac{T_D}{T_{\max}} \tag{72}$$

where

$$T_{\max} = (z\gamma_b + q)K(S_v \times S_h) \tag{73}$$

z = depth of the reinforcement layer from the top of the RSW height; $S_v = (H_2/n)$; $S_h = 1$ m; $K = T_{r\max}/0.5\gamma_b H_2^2$ is the reinforcement force coefficient; n = number of reinforcement layers; and $T_{r\ \max}$ = maximum tensile strength of the reinforcement. Furthermore, $T_{r\ \max}$ can be obtained by maximizing the value of T_r (Basha and Babu 2011), as mentioned subsequently.

Table 3. Deterministic parameters considered in this study

Deterministic parameters	Values
B_2/H_2	0.55–1.00
H_2/H_1	0.10–0.20
H_t/H_1	0.0–0.5
B_t/H_1	0.15
ξ	14°
ψ	18.43°
η	9°–18°
θ	1.1°
N	5–35

Find θ_1 and θ_2 that

$$\begin{cases}\text{maximize} & T_r\\ \text{subjected to} & \begin{cases}0^\circ < \theta_1 < 90^\circ\\ 0^\circ < \theta_2 < 90^\circ\end{cases}\end{cases} \tag{74}$$

The values of T_D and $T_{\max}$ in Eq. (72) are normalized by $\gamma_b H_2^2$ to compute FS_t, which is further termed T_{D_N} and $T_{\max\_N}$. These expressions are given as follows:

$$T_{D\_N} = \frac{T_D}{\gamma_b H_2^2} \tag{75}$$

$$T_{\max\_N} = \frac{T_{\max}}{\gamma_b H_2^2} \tag{76}$$

The long-term design reinforcement strength (T_D) can be evaluated from the ultimate reinforcement strength of the geosynthetic with the implementation of reduction factors for phenomena such as installation damage, creep, and biological/chemical degradation. The present study considers the requisite geosynthetic force for the stabilization of an RSW a random variable, unlike using the conventional reduction factors. The probabilistic constraint as the performance function for the tensile failure mode is expressed as follows:

$$g_t = FS_t - 1 \le 0 \tag{77}$$

Factor of Safety against Pullout Failure

Factor of safety against pullout resistance is the ratio of available resisting force (P_{ri}) acting on the embedded length of the

Table 4. Mean and COVs of input parameters considered in the study

		Statistics		
Random variable	Mean	COV (%)	Distribution	Source
γ_{sw} (kN/m^3)	10.2	10	Normal	Singh et al. (2009)
ϕ_{sw} (°)	30	10	Lognormal	Singh et al. (2009)
c_{sw_N}	0.06	10	Lognormal	Babu et al. (2014)
δ_{12} (°)	16	10	Lognormal	Sia and Dixon (2007)
c_{1_N}	0.40	10	Lognormal	Babu et al. (2014)
c_{2_N}	0.20	10	Lognormal	Babu et al. (2014)
γ_b (kN/m^3)	18	5	Normal	Duncan (2000)
c_{b_N}	0.15	10	Lognormal	Phoon and Kulhawy (1999)
ϕ_b (°)	30	10	Lognormal	Phoon and Kulhawy (1999)
γ_s (kN/m^3)	19	5	Normal	Duncan (2000)
c_{s_N}	0.03	10	Lognormal	Duncan (2000)
ϕ_s (°)	32	10	Lognormal	Phoon and Kulhawy (1999)
δ_b (°)	$(2/3)\phi_s$	10	Lognormal	Phoon and Kulhawy (1999)
δ_{br} (°)	20	10	Lognormal	Phoon and Kulhawy (1999)
T_{D_N}	0.02–0.08	0–10	Normal	Chalermyanont and Benson (2004)

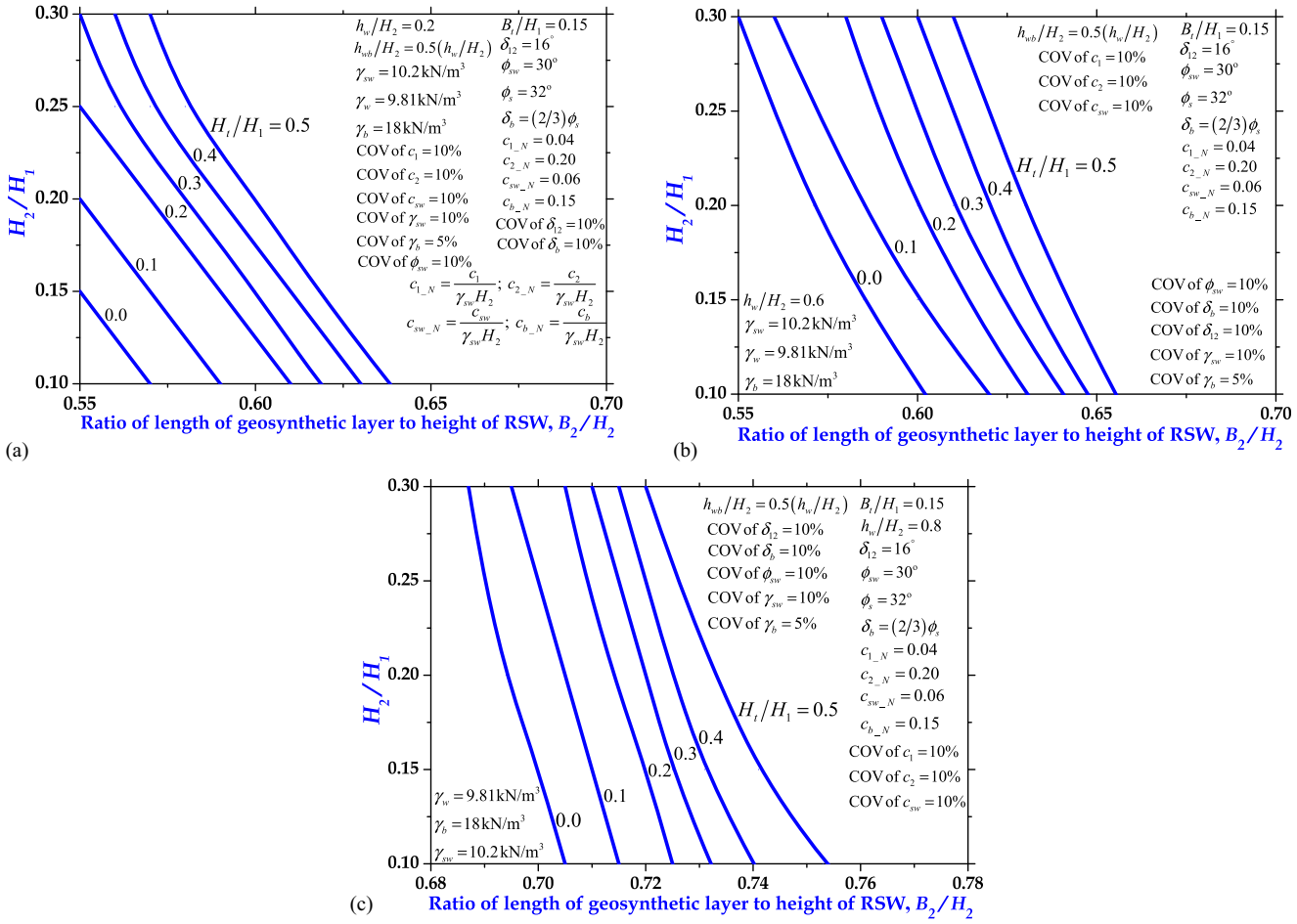

Fig. 4. Influence of (H_t/H_1) and (H_2/H_1) on the length of a geosynthetic layer to stabilize an RSW (B_2/H_2) in Case 1 condition for $\beta_{lb} = 3.0$: (a) $h_w/H_2 = 0.2$; (b) $h_w/H_2 = 0.6$; and (c) $h_w/H_2 = 0.8$.

reinforcement (L_e) to the maximum possible load in the soil reinforcement ($T_{\max}$), as shown in Fig. 3(b), which is given as follows:

$$FS_{po} = \frac{P_{ri}}{T_{\max}} \tag{78}$$

where $P_{ri} = 2\sigma_{vi}L_e \tan\delta_{br}$; δ_{br} = minimum interface friction angle between geosynthetics and reinforced soil; and $\sigma_{vi} = z\gamma_b$ is the effective vertical stress acting on the embedded reinforcement length (L_e). The pullout resistance at the top is used to estimate the length of reinforcement. Further, the values of P_{ri} and $T_{\max}$ in Eq. (78) are normalized by $\gamma_b H_2^2$ to find FS_{po}. The normalized values of P_{ri} and $T_{\max}$ are termed P_{ri_N} and $T_{\max\_N}$. The probabilistic constraint as the performance function for the pullout failure mode is written as follows:

$$g_{po} = FS_{po} - 1 \le 0 \tag{79}$$

Validation of Methodology for Different Leachate Buildup Cases

The methodology proposed in this study has been validated by Qian (2008) for different leachate buildup conditions. Qian (2008) reported the buildup of leachate for a landfill without an RSW or a retaining structure (used two-wedge failure mechanism). Therefore, to validate the present analysis, the dimensions of an MSW landfill with an RSW have been modified considering $u = 0^\circ$ and $\alpha = 0^\circ$ [refer to Figs. A5(a and b)]. Table 1 provides a comparison of the factors of safety obtained using the present study with those obtained from Qian (2008). The following four leachate buildup conditions have been studied: seepage buildup parallel to the back slope and subgrade; seepage buildup parallel-to-subgrade; horizontal seepage buildup along with seepage parallel to the back slope; and horizontal seepage buildup. The chosen parameters for validating the present methodology are given in Table 2. Table 1 provides marginal differences of about 2% between the factors of safety obtained using the present study and those obtained using Qian (2008). This can be attributed to the conversion of the present three-wedge mechanism to a two-wedge mechanism. It confirms the validity of the present formulation.

Results and Discussion

The deterministic range of parameters used in the analysis is given in Table 3. The mean values of input parameters and the coefficient of variations (COVs) of random parameters are provided in Table 4.

The design charts, Figs. 4(a–c), 5(a–c), 6(a–c), 7(a–c), 8(a–c), and 9(a–c), are presented for three different leachate buildup levels in an MSW landfill with respect to the height of an RSW (h_w/H_2) for six cases individually discussed in the previous sections. The three different leachate levels, h_w/H_2, are 0.2, 0.6, and 0.8. Figs. 10(a and b) and 11–13 illustrate the effect of the tensile

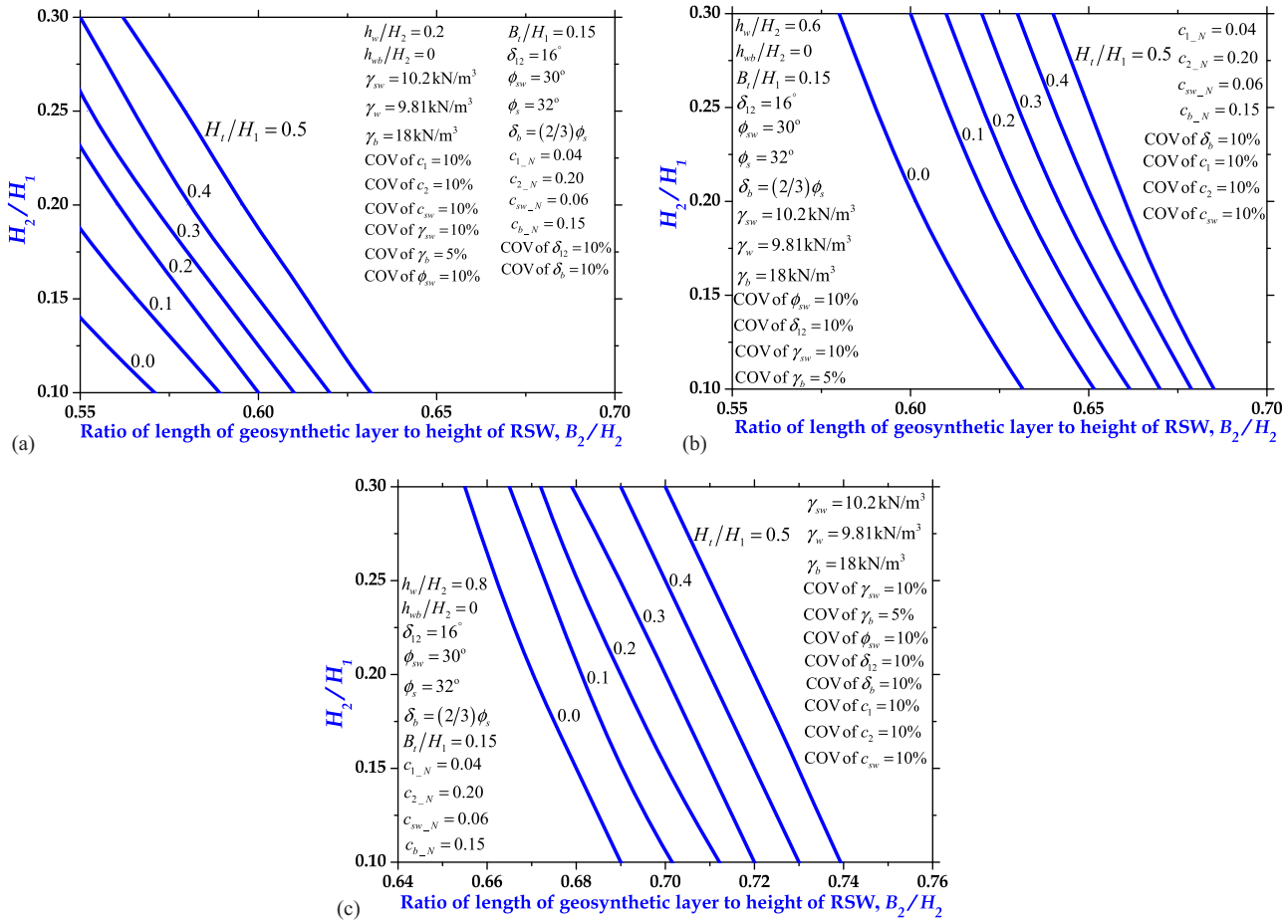

Fig. 5. Influence of (H_t/H_1) and (H_2/H_1) on the length of a geosynthetic layer to stabilize an RSW (B_2/H_2) in Case 2 condition for $\beta_{lb} = 3.0$: (a) $h_w/H_2 = 0.2$; (b) $h_w/H_2 = 0.6$; and (c) $h_w/H_2 = 0.8$.

strength of the geosynthetic (T_{D_N}) and the number of geosynthetic layers (n) against tension as well as pullout failures. Table 3 provides the optimum values of the length of reinforcement to the height of the RSW (B_2/H_2) and the number of reinforcement layers (n) for Cases 5 and 6 against external and internal modes of failure.

Influence of Leachate Head h_w/H_2 and Vertical Expansion of an MSW Landfill (H_t/H_1) on the Design of an RSW under Case 1

Figs. 4(a and b) present the optimum dimensions of an RSW, that is H_2/H_1 and B_2/H_2 corresponding to different vertically expanded heights of an MSW landfill (H_t/H_1) for Case 1 and $h_w/H_2 = 0.2$, 0.6, and 0.8. The results shown in Figs. 4(a–c) indicate that the H_2/H_1 needs to be increased with an increase in h_w/H_2 for a constant value of B_2/H_2 in Case 1, when $h_{wb}/H_2 = 0.5(h_w/H_2)$, and for a system reliability index (β_{lb}) of 3.0. In Case 1, as shown in the figures, the magnitude of B_2/H_2 for any value of H_t/H_1 and H_2/H_1 increases rapidly when the level of leachate (h_w/H_2) increases from 0.2 to 0.8. Therefore, it is important to select the adequate ratios of the length of geosynthetic reinforcement to the height of an RSW and the height of an RSW to the height of a landfill under different leachate levels (h_w/H_2) to safeguard against the translational failure of an RSW for a vertically expanded MSW landfill.

It is observed that B_2/H_2 increases from 0.590 to 0.725 when h_w/H_2 increases from 0.2 to 0.8 for $H_t/H_1 = 0.4$ and $H_2/H_1 = 0.2$, as depicted in Figs. 4(a–c). It has been noted from Fig. 4(a) that B_2/H_2 increases from 0.550 to 0.618 with an increase in the value of H_t/H_1 from 0.0 to 0.5 for $H_2/H_1 = 0.15$ and $h_w/H_2 = 0.2$. In addition, B_2/H_2 reduces from 0.640 to 0.590 with an increase in H_2/H_1 value from 0.10 to 0.30 for $H_t/H_1 = 0.3$ and $h_w/H_2 = 0.6$, as illustrated in Fig. 4(b). Therefore, as the value of h_w/H_2 increases, the ratio of B_2/H_2 should be increased to maintain the target value of the reliability index (β_{lb}) of 3.0.

Influence of h_w/H_2 and Vertical Expansion of an MSW Landfill (H_t/H_1) on the Design of an RSW under Case 2

The results illustrated in Figs. 5(a–c) demonstrate the influence of seepage flow parallel to subgrade on the design parameters of an RSW for three different leachate levels, $h_w/H_2 = 0.2$, 0.6, and 0.8. The design charts for Case 2 are demonstrated to evaluate the safe design parameters of the RSW (H_2/H_1 and B_2/H_2) under different expanded heights (H_t/H_1) of an MSW landfill for two leachate levels (h_w/H_2). From Figs. 5(a–c), it can be illustrated that for a given h_w/H_2, the value of B_2/H_2 increases considerably with an increase in the value of H_t/H_1 from 0.0 to 0.5. For example, B_2/H_2 increases from 0.545 to 0.614 when H_t/H_1 increases from 0.0 to 0.5 for $H_2/H_1 = 0.15$ and $h_w/H_2 = 0.2$ [refer to Fig. 5(a)]. From Figs. 5(a–c), it has been investigated that the value of B_2/H_2 increases significantly as the value of H_2/H_1 reduces from 0.30 to 0.10 for constant values of H_t/H_1 and h_w/H_2. It is observed from the results illustrated in Figs. 5(a–c) that B_2/H_2 reduces rapidly from 0.610 to 0.540 (for $h_w/H_2 = 0.2$), from 0.670 to 0.620 (for $h_w/H_2 = 0.6$), and from 0.720 to 0.679 (for $h_w/H_2 = 0.8$) when H_2/H_1 increases from 0.10 to 0.3 and H_t/H_1 is 0.3. The design

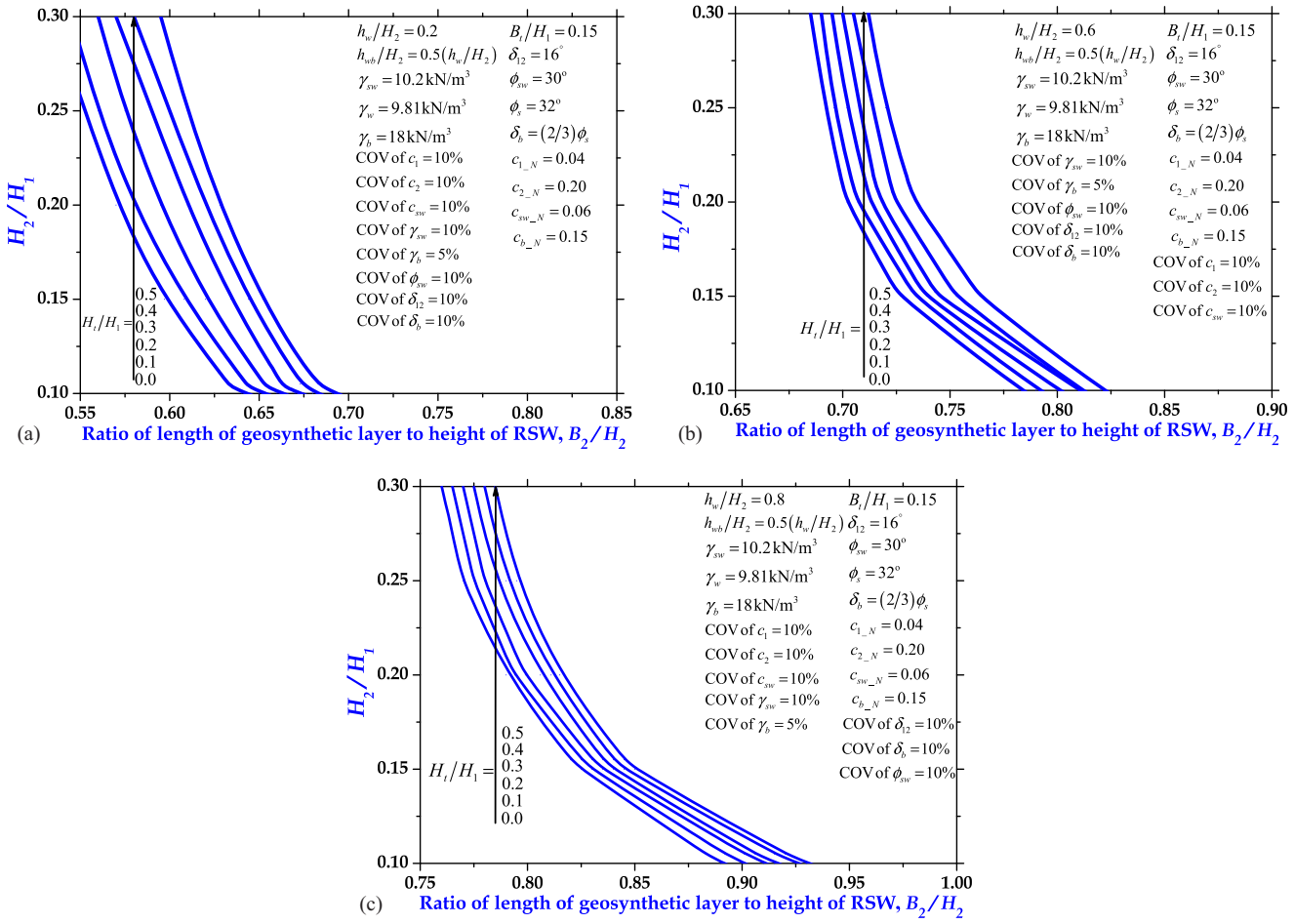

Fig. 6. Influence of (H_t/H_1) and (H_2/H_1) on the length of a geosynthetic layer to stabilize an RSW (B_2/H_2) in Case 3 condition for $\beta_{lb} = 3.0$: (a) $h_w/H_2 = 0.2$; (b) $h_w/H_2 = 0.6$; and (c) $h_w/H_2 = 0.8$.

length of reinforcement should be increased to maintain the static safety levels when h_w/H_2 increases from 0.2 to 0.8. It is clear from Fig. 5(c) that B_2/H_2 for the expanded height of the landfill should be higher in magnitude for $h_w/H_2 = 0.8$ and $h_{wb}/H_2 = 0$.

Influence of h_w/H_2 and Vertical Expansion of an MSW Landfill (H_t/H_1) on the Design of an RSW under Case 3

The influence of the buildup of horizontal seepage along with seepage parallel to the back slope condition on assessing the optimum dimensions of an RSW is shown in Figs. 6(a–c). It can be noted that as the magnitude of H_2/H_1 increases, B_2/H_2 decreases for a constant expanded height of an MSW landfill (H_t/H_1). The desired length of the geosynthetic reinforcement (i.e. B_2/H_2 ranging from 0.640 to 0.691) is greater than that of the previous case (i.e. B_2/H_2 ranging from 0.570 to 0.638 as shown in Fig. 4(a)), when $Ht/H1$ increases from 0.0 to 0.5 for $hw/H_2 = 0.2$, $hwb/H_2 = 0.5$ (hw/H_2), $H_2/H_1 \leq 0.10$, and $\beta lb = 3.0$. This helps maintain the static stability of the RSW for a constant value of H_2/H_1. In addition, for a constant value of H_t/H_1 (e.g., 0.2), $h_w/H_2 = 0.8$, and for a higher H_2/H_1 value of (e.g., 0.25), the desired length of the geosynthetic should be lower (e.g., 0.780) to make the construction of the RSW economical and safe. In contrast, for a constant value of H_t/H_1 (e.g., 0.2), $h_w/H_2 = 0.8$, and for a lower H_2/H_1 value (e.g., 0.10), the desired length of the geosynthetic should be higher (e.g., 0.910) to maintain the external stability of the RSW. For constant values of $H_2/H_1 = 0.2$ and $H_t/H_1 = 0.5$, B_2/H_2 increases from 0.628 to 0.815 to maintain the safety levels with an increase in h_w/H_2 from 0.2 to 0.8. Therefore, it can be noted that a higher leachate level within the MSW landfill increases the required length of geosynthetic reinforcement (B_2/H_2), as illustrated in the figures.

Influence of h_w/H_2 and Vertical Expansion of an MSW Landfill (H_t/H_1) on the Design of an RSW under Case 4

In this section, the safe design parameters of an RSW are evaluated for different values of h_w/H_2 under horizontal seepage buildup conditions. It is observed from Figs. 7(a–c) that the magnitude of B_2/H_2 increases with an increase in h_w/H_2 values from 0.2 to 0.8. For example, $B_2/H_2 = 0.638$, $B_2/H_2 = 0.740$, and $B_2/H_2 = 0.829$ for $H_2/H_1 = 0.15$ and $H_t/H_1 = 0.4$ as h_w/H_2 increases from 0.2 to 0.8, respectively [Figs. 7(a–c)]. It may be noted from Figs. 7(a–c) that for constant values of B_2/H_2 and H_t/H_1, the magnitude of H_2/H_1 increases significantly with an increase in h_w/H_2 from 0.2 to 0.8.

It can be noted from Fig. 7(c) that for constant values of $h_w/H_2 = 0.8$ and $H_t/H_1 = 0.2$, B_2/H_2 varies from 0.890 to 0.746 when H_2/H_1 increases from 0.10 to 0.30. It can be noted from the design charts that for a target value of reliability index $(\beta_{lb} = 3.0)$, H_2/H_1 and B_2/H_2 need to be increased to ensure stability against three external failure modes during the vertical expansion of an MSW landfill with an increase in the magnitude of leachate heads (h_w/H_2) from 0.2 to 0.8.

Int. J. Geomech., 2023, 23(4): 04023027

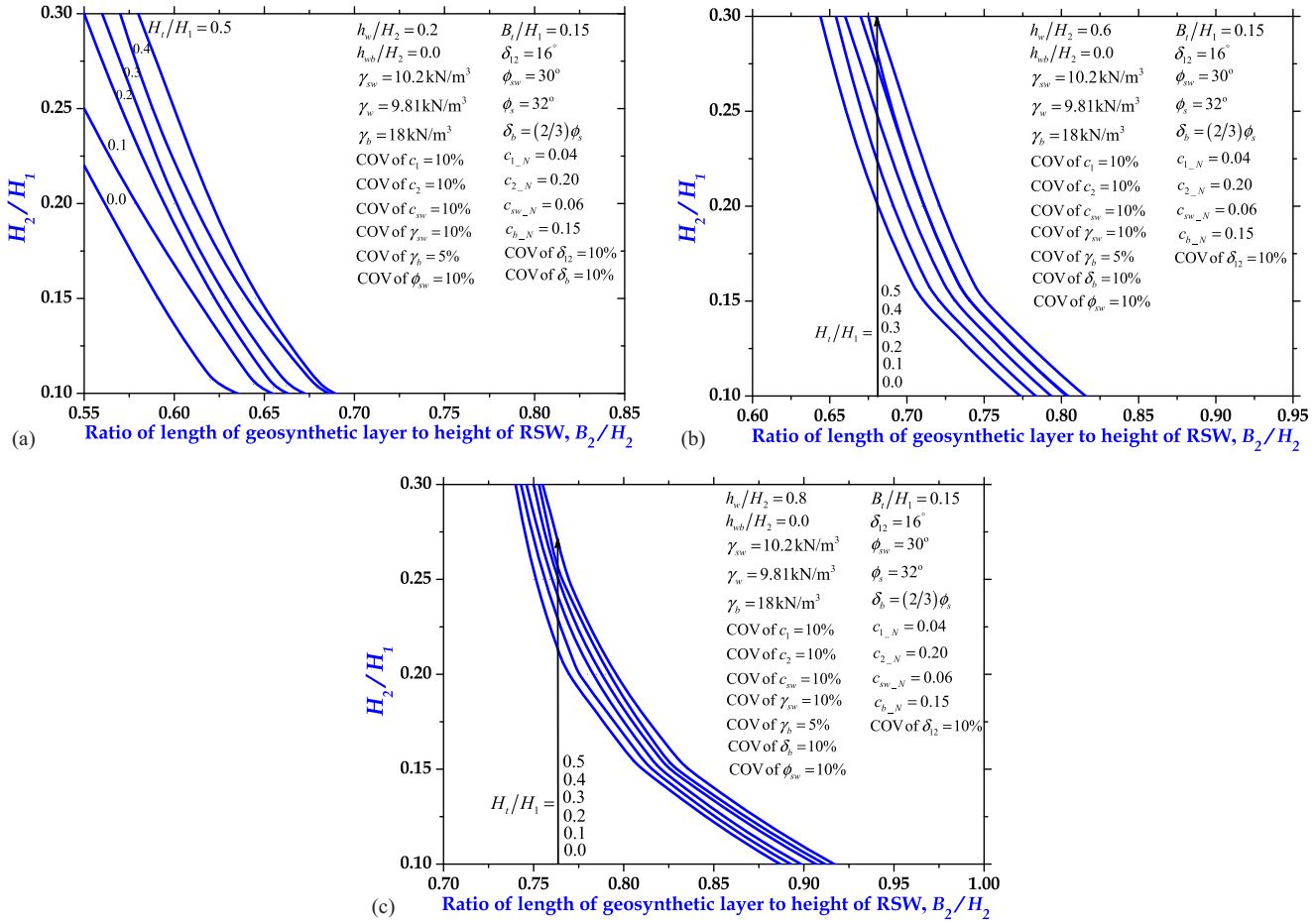

Fig. 7. Influence of (H_t/H_1) and (H_2/H_1) on the length of a geosynthetic layer to stabilize an RSW (B_2/H_2) in Case 4 condition for $\beta_{lb} = 3.0$: (a) $h_w/H_2 = 0.2$; (b) $h_w/H_2 = 0.6$; and (c) $h_w/H_2 = 0.8$.

Influence of h_w/H_2 and Vertical Expansion of an MSW Landfill (H_t/H_1) on the Design of an RSW under Case 5

Figs. 8(a–c) show the design charts for estimating the optimum dimensions of an RSW when the leachate flow is parallel to the front slope and back slope of the landfill condition for a typical set of parameters. This case may represent the ideal condition in any MSW landfill with an RSW, in which leachate is being efficiently collected by the leachate collection system, and there is no leachate buildup behind the RSW. The results presented in Figs. 8(a–c) report that for a given value of $H_2/H_1 = 0.10$, B_2/H_2 rises from 0.550 to 0.610 (for $h_w/H_2 = 0.2$), from 0.570 to 0.630 (for $h_w/H_2 = 0.6$), and from 0.580 to 0.640 (for $h_w/H_2 = 0.8$) when H_t/H_1 increases from 0.0 to 0.5.

Fig. 8(a) shows that for $H_t/H_1 = 0.4$, $h_w/H_2 = 0.2$, and $h_{wb}/H_2 = 0.5(h_w/H_2)$, the ratio of B_2/H_2 reduces from 0.600 to 0.550 when H_2/H_1 increases from 0.10 to 0.30. Further, from Fig. 8(c), it can be found that B_2/H_2 reduces from 0.620 to 0.580 when H_2/H_1 increases from 0.10 to 0.30 for $H_t/H_1 = 0.4$, $h_w/H_2 = 0.8$, and $h_{wb}/H_2 = 0.5(h_w/H_2)$. Hence, the optimum dimensions of an RSW can be obtained against failure in bearing capacity, sliding, and eccentricity. The optimum design values of an RSW are reported in the design charts for $\beta_{lb} = 3.0$.

Influence of h_w/H_2 and Vertical Expansion of an MSW Landfill (H_t/H_1) on the Design of an RSW under Case 6

The results presented in Figs. 9(a–c) pertain to the optimum dimensions of an RSW for a vertically expanded MSW landfill when the leachate flow is parallel to the front slope of the landfill. The design charts are developed for different values of h_w/H_2 and for $\beta_{lb} = 3.0$. This is one of the suitable cases after Case 5, where the leachate collection system installed in the landfill collects and removes the leachate. Hence, there is no leachate buildup against the RSW. Figs. 9(a–c) show the influence of h_w/H_2, which ranges from 0.2 to 0.8 on the lower-bound solution of the system reliability index against external failure modes. It is clear from Fig. 9(a) that for $H_2/H_1 = 0.1$, the optimum length of the reinforcement layer (B_2/H_2) needs to be increased from 0.545 to 0.610 when H_t/H_1 increases from 0.0 to 0.5, $h_w/H_2 = 0.2$, and $h_{wb}/H_2 = 0.0$. Hence, the ratio of B_2/H_2 increases with an increase in the ratio of H_t/H_1 for a constant leachate buildup level and for a constant ratio of H_2/H_1. It is observed from Figs. 9(a–c) that for $H_t/H_1 = 0.5$ and $H_2/H_1 = 0.3$, B_2/H_2 is 0.550 for $h_w/H_2 = 0.2$, 0.565 for $h_w/H_2 = 0.6$, and 0.580 for $h_w/H_2 = 0.8$. It is found from the figures that for $h_w/H_2 = 0.8$, the required ratio of B_2/H_2 is more than that of $h_w/H_2 = 0.2$ to maintain the stability of the system against external failure modes. Hence, the suitable dimensions of the RSW should be provided with an increase in the value of the leachate head (h_w/H_2) from 0.2 to 0.8.

Effect of T_{D_N} and COV of T_D on β_t

Fig. 10(a) shows the influence of the normalized tensile strength of geosynthetic reinforcement (T_{D_N}) and number of reinforcement layers (n) for a COV of $T_D = 5\%$ on the reliability index against tensile failure (β_t) when $T_{D\_N} = 0.02$–0.08, $\gamma_b = 18$ kN/m^3, $\phi_b = 30^\circ$, and

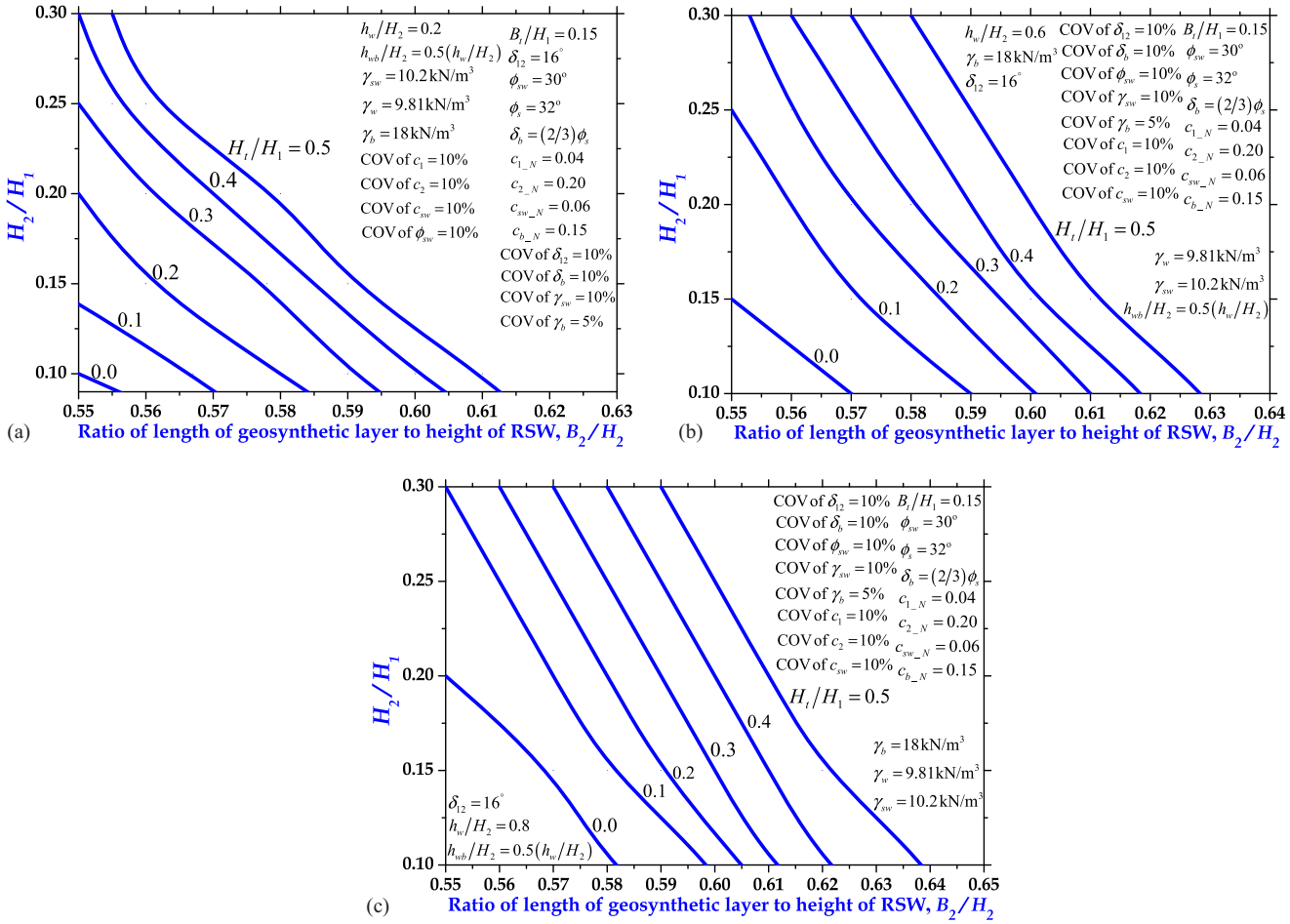

Fig. 8. Influence of (H_t/H_1) and (H_2/H_1) on the length of a geosynthetic layer to stabilize an RSW (B_2/H_2) in Case 5 condition for $\beta_{lb} = 3.0$: (a) $h_w/H_2 = 0.2$; (b) $h_w/H_2 = 0.6$; and (c) $h_w/H_2 = 0.8$.

$\delta_{br}/\phi_b = 1$ and a COV of γ_b, ϕ_b, and δ_{br} = 5%, 10%, and 10%, respectively. It can be reported that the number of geosynthetic layers (n) can be reduced for a given fixed value of the target reliability index (β_t) when T_{D_N} increases from 0.02 to 0.08. Fig. 10(a) indicates that β_t increases with the rise in n values for a constant value of T_{D_N}. For $\beta_t = 3.0$ and $H_2/H_1 = 0.1$, the number of geosynthetic layers (n) required for the design of the RSW for $T_{D\_N} = 0.02$, 0.04, and 0.06 is 20, 10, and 6, respectively. The COV of normalized tensile strength of reinforcement (COV of T_D) exhibits a great effect on the number of reinforcements (n). Based on the results from Figs. 10(a and b), it is noted that β_t decreases significantly with an increase in the values of COV of T_D from 5% to 10%. An observation that can be made from Figs. 10(a and b) is that for $\beta_t = 3.0$, the number of reinforcement layers (n) required to be accommodated during the construction of the RSW for the constant tensile strength of reinforcement T_{D_N}; = 0.04 is 10 and 11 for a COV of $T_D = 5\%$ and 10%, respectively. It is evident from this discussion that the variability associated with the tensile strength of reinforcement (T_D) influences the reliability index against tensile stress (β_t) considerably, and it should be given due consideration to obtain a suitable number of geosynthetic layers for the safe design of an RSW.

Effect of n *and* B_2/H_2 *on the Reliability Index against Pullout Failure* (β_{po})

This section deals with the estimation of the length of geosynthetic reinforcement in relation to the height of the RSW (B_2/H_2) against the different numbers of reinforcements (n). Fig. 11 provides the suitable design ratio, B_2/H_2, to ensure stability against failure in pullout mode for the chosen value of the number of reinforcements (n), δ_{br}/ϕ_b = 2/3, and a COV of δ_{br} = 10%. It can be noted that the ratio of B_2/H_2 decreases marginally with an increase in the number of geosynthetic reinforcement layers (n). For example, the ratio B_2/H_2 reduces from 0.63 to 0.56 when n increases from 5 to 35 to achieve the target reliability index against a pullout failure (β_{po}) of 3.0. In addition, for a constant n value, the reliability index against pullout failure (β_{po}) increases with an increase in the length of geosynthetic reinforcement to a height of RSW ratio (B_2/H_2).

Design of an RSW for System Stability

Fig. 12 gives the values of the number of reinforcement layers (n) for different magnitudes of the lower-bound value of the system reliability index (β_{lb}), B_2/H_2 ratios, $T_{D\_N} = 0.02$–0.04, and a COV of $T_D = 5\%$. For a design value of B_2/H_2, obtained from the external stability of the RSW, the number of reinforcement layers (n) needs to be obtained to ensure the internal stability of the RSW. It can be noted that for a given value of B_2/H_2, β_{lb} rises with an increase in the number of layers (n). The tensile strength of reinforcement (T_{D_N}) influences the number of geosynthetic layers considerably. An observation that can be made from the figures is that for $\beta_{lb} = 3.0$ and a COV of $T_D = 5\%$, the minimum number of reinforcements (n) required is 21 and 10 for $T_{D\_N} = 0.02$ and

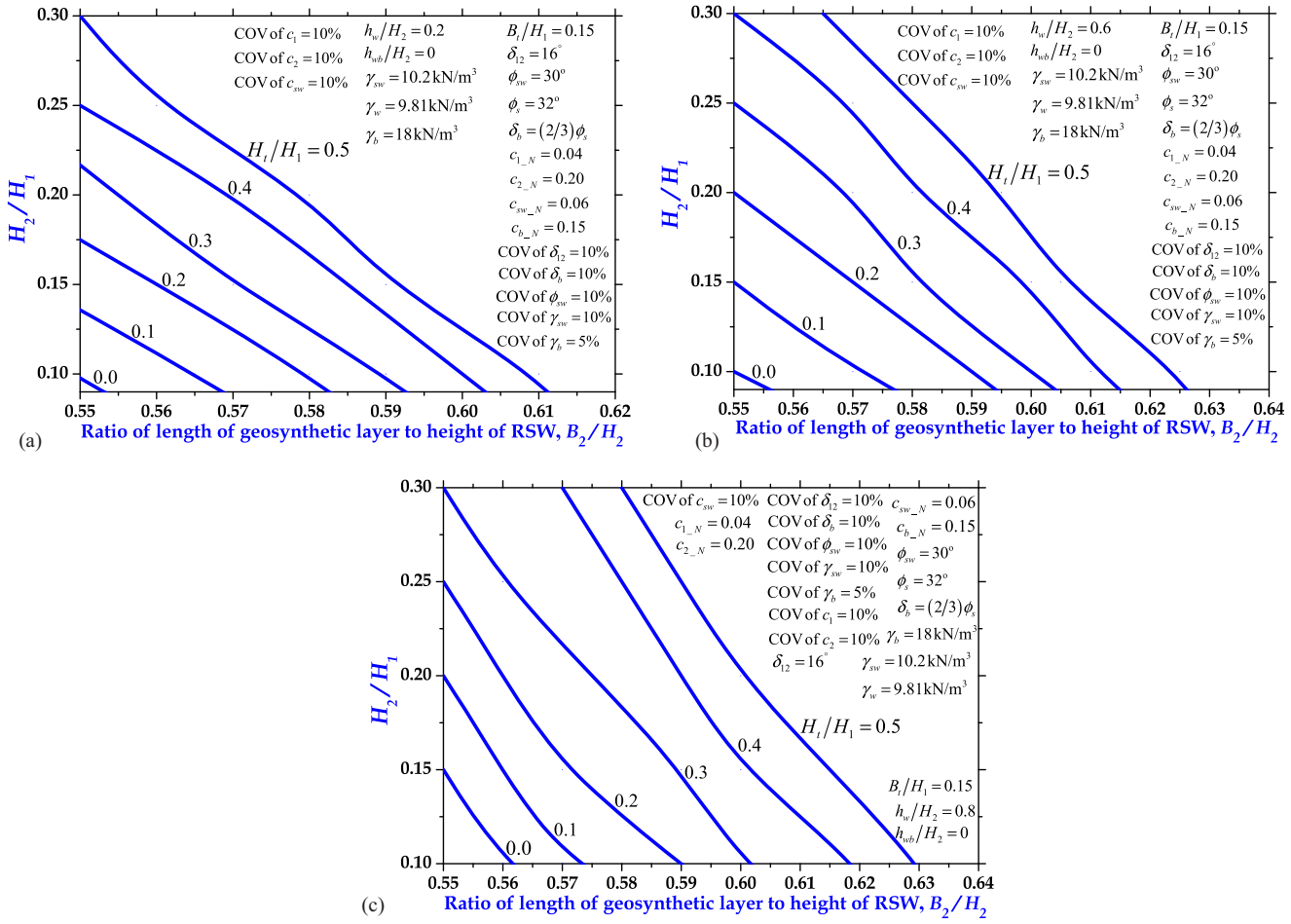

Fig. 9. Influence of (H_t/H_1) and (H_2/H_1) on the length of a geosynthetic layer to stabilize an RSW (B_2/H_2) in Case 6 condition for $\beta_{lb} = 3.0$: (a) $h_w/H_2 = 0.2$; (b) $h_w/H_2 = 0.6$; and (c) $h_w/H_2 = 0.8$.

0.04, respectively. This trend of results may not be the same for other sets of input parameters. Considering the importance of the structure, the number of reinforcement layers can be increased accordingly. The strength (T_{D_N}) and the number of reinforcement layers (n) should be chosen cautiously to maintain the stability of the RSW against internal modes of failure. The design charts are useful for determining the number of reinforcement layers corresponding to the design strength of geosynthetic reinforcement used in the construction of the RSW and the already estimated design values of the length of reinforcement to the height of RSW ratio necessary to stabilize the RSW against all three external modes of failure.

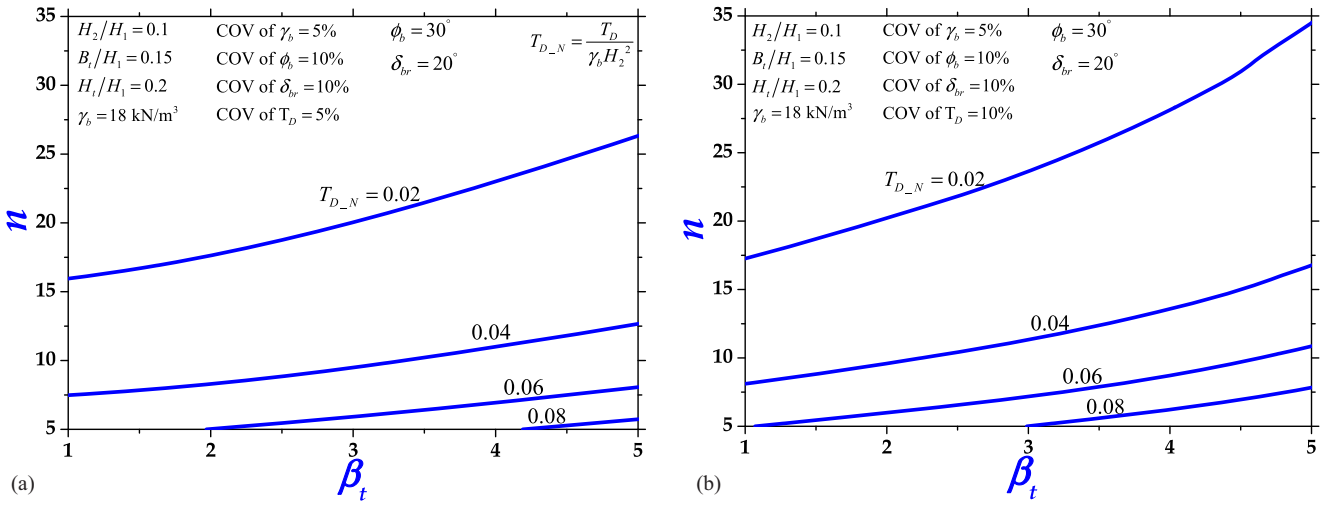

Fig. 10. Influence of the tensile strength of the geosynthetic (T_{D_N}) and number of geosynthetic layers (n) on the reliability index against tension failure (β_t) for (a) COV of $T_D = 5\%$; and (b) COV of $T_D = 10\%$.

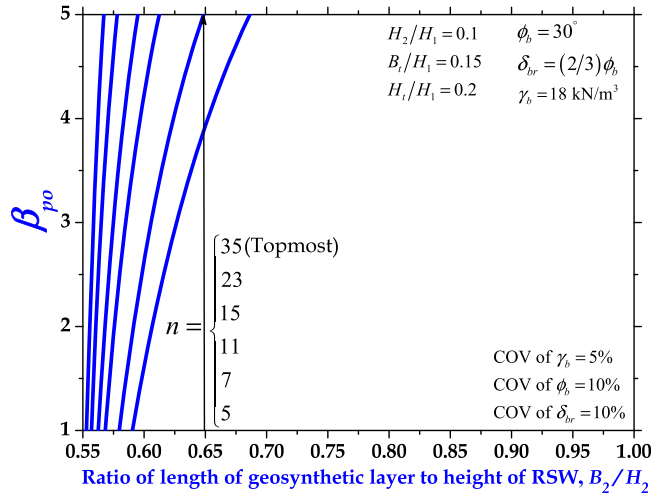

Fig. 11. Relationship between B_2/H_2 and the reliability index against pullout failure (β_{po}) with various values of n.

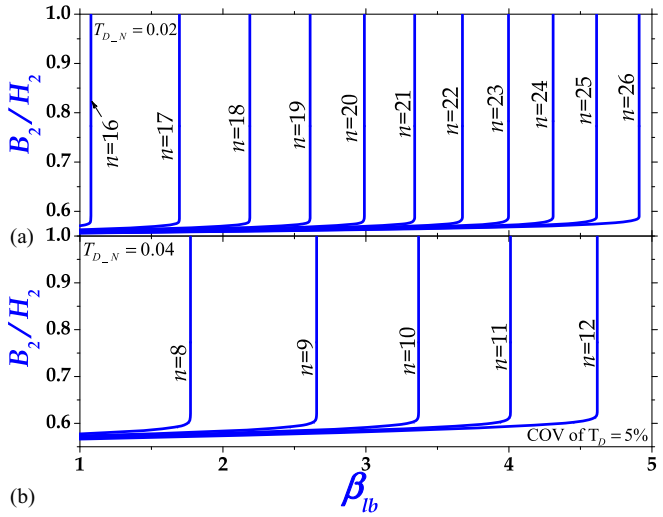

Fig. 12. Relationship between B_2/H_2 and the lower bound of the system reliability index (β_{lb}) with various values of n and a COV of T_D = 5% for (a) $T_{D\_N} = 0.02$; and (b) $T_{D\_N} = 0.04$.

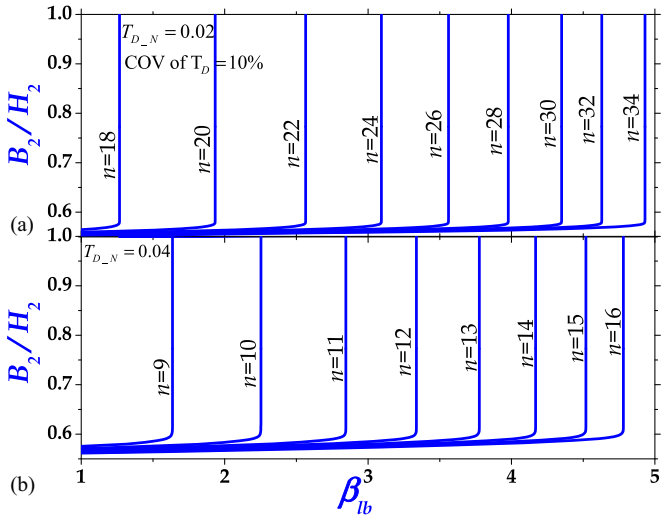

Fig. 13. Relationship between B_2/H_2 and the lower bound of the system reliability index (β_{lb}) with various values of n and a COV of T_D = 10% for (a) $T_{D\_N} = 0.02$; and (b) $T_{D\_N} = 0.04$.

For this reason, Fig. 13 is plotted to obtain the number of layers (n) for the predetermined ratio of B_2/H_2 from external stability analysis, design tensile strength (T_{D_N} varies from 0.02 to 0.04) of geosynthetic reinforcement, and variability associated with the design strength (a COV of T_D). Based on the plotted results, it can be illustrated that the number of reinforcements (n) should be increased as the COV of T_D rises from 5% to 10%. For example, the number of layers required for $T_{D\_N} = 0.04$ and the target value of $\beta_{lb} = 3.0$ is 10 and 12 for a COV of T_D = 5% and 10%, respectively.

Optimum Values of the Number of Layers and B_2/H_2 under Leachate Buildup Conditions

The optimum values of the length of the reinforcement to a height of an RSW (B_2/H_2) and the number of layers (n) can be obtained for different leachate buildup levels for two cases considered in this study, that is (a) parallel-to-front slope of landfill and back slope seepage buildup as discussed in Case 5, and (b) parallel-to-front slope of landfill seepage buildup as discussed in Case 6. Table 5 is useful for obtaining the optimum design values of B_2/H_2 and

Table 5. Design values of n and B_2/H_2 for a system reliability index (β_{lb}) of 3.0, COV of T_D = 5% and 10%, and Cases 5 and 6

			Internal stability analysis					Design values of B_2/H_2 and n (maximum value of B_2/H_2 from external and internal stability)			
				$T_{D\_N} = 0.02$		$T_{D\_N} = 0.04$		$T_{D\_N} = 0.02$		$T_{D\_N} = 0.04$	
Cases considered in the study	COV of T_D (%)	$\frac{h_w}{H_2}$	B_2/H_2	B_2/H_2	n	B_2/H_2	n	B_2/H_2	n	B_2/H_2	n
Case 5	5	0.2	0.58	0.57	21	0.59	10	0.58	21	0.59	10
		0.6	0.60					0.60		0.60	
		0.8	0.61					0.61		0.61	
Case 6		0.2	0.58	0.57	21	0.59	10	0.58	21	0.59	10
		0.6	0.59					0.59		0.59	
		0.8	0.59					0.59		0.59	
Case 5	10	0.2	0.58	0.57	24	0.59	12	0.58	24	0.59	12
		0.6	0.60					0.60		0.60	
		0.8	0.61					0.61		0.61	
Case 6		0.2	0.58	0.57	24	0.59	12	0.58	24	0.59	12
		0.6	0.59					0.59		0.59	
		0.8	0.59					0.59		0.59	

the number of layers (n). The leachate collection system provided in the MSW landfill takes care of the collection and removal of leachate. The strength and geometric properties of MSW and the RSW used in the analysis are as follows: $\phi_{sw} = 30°$, $c_{sw\_N} = 0.06$, $c_{1\_N} = 0.04$, $c_{2\_N} = 0.20$, $c_{b\_N} = 0.15$, $\phi_b = 30°$, $\phi_s = 32°$, $\delta_{12} = 16°$, $\delta_b = (2/3)\phi_s$, $H_2/H_1 = 0.1$, $H_t/H_1 = 0.2$, $B_t/H_1 = 0.15$, $L_1/H_1 = 2.2$, $\eta = 14.35°$, $\theta = 1.1°$, $\psi = 18.43°$, and $\xi = 14°$. It can be observed from the results presented in the tables that as the value of the COV of T_D increases, the number of reinforcement layers needs to be increased to maintain the internal stability of the RSW. For example, for $T_{D\_N} = 0.04$, the number of reinforcement layers (n) increases from 10 to 12 as the COV of T_D increases from 5% to 10%.

It is recommended to provide the optimum ratio of reinforcement length to wall height (B_2/H_2) ranges from 0.58 to 0.61. The number of reinforcement layers ranges from 10 to 24, as given in Table 5, when the leachate head (h_w/H_2) ranges from 0.2 to 0.8, the normalized design strength of geosynthetic reinforcement (T_{D_N}) ranges from 0.02 to 0.04, and the COV of T_D ranges from 5% to 10% to satisfy the external and internal stability modes simultaneously. An important observation that can be made from this study is that the minimum length of the reinforcement is $0.58H_2$, which is much less than the minimum length requirement of $0.7H_2$ as suggested by FHWA (2001). This can be attributed to the fact that the magnitude of waste pressure that is acting on an RSW due to waste mass as backfill material is much less than the active earth pressure resulting from conventional backfill materials. Landva et al. (2000) reported that the reduction in at-rest waste pressure is due to the amount of fibrous contents in the waste mass. Zhang et al. (2013) compared the soil and waste pressures during excavation on the basis of in situ observations and concluded that the reduced value of waste pressure is due to the high magnitude of shear strength of MSW because of the high amount of fiber content.

Conclusions

This study gives a design methodology for the series system reliability assessment of RSWs subjected to six leachate buildup conditions by considering the dependency between the external and the internal stability modes of failure. A formulation is presented to estimate the PWPs for all six leachate buildup conditions. It is observed that the leachate flow parallel to the front slope and back slope of the landfill (referred to Case 5) may be an ideal condition when the RSW exists in front of the MSW landfill. This assumption causes no leachate buildup behind the RSW. Additionally, the leachate flow is considered as parallel to the front slope of the landfill (referred to Case 6) when the leachate collection system functions properly. This means that it collects and removes the leachate. The main findings of the present investigation are as follows:

1. It is demonstrated that the length of geosynthetic reinforcement to a height of RSW ratio (B_2/H_2) needs to be increased significantly with the rise in leachate levels (h_w/H_2) from 0.2 to 0.8 for a target value of a system reliability index of 3.0 for all the six leachate buildup cases. Hence, the leachate levels are an important aspect in the design of RSWs.
2. It is found that the required ratio of geosynthetic reinforcement length to RSW height (B_2/H_2) for any value of H_t/H_1 is more in case of a buildup of horizontal seepage along with seepage parallel to the back slope (Case 3). Hence, Case 3 is the most critical case among all the six cases of leachate buildup.
3. The optimum number of geosynthetic layers (n) for different normalized tensile strengths of geosynthetic reinforcement (T_{D_N}) is proposed to maintain the reinforced soil wall safe against tension failure (β_t). It is observed that the design strength of the reinforcement (T_D) has a noticeable effect on the reliability index against failure in tension in the internal stability analysis of the RSW.
4. The influence of tension failure and pullout failure is considered in evaluating the system reliability index. Additionally, the lower bound of system reliability (β_{lb}) is used for the conservative design.
5. The COV of design reinforcement strength (T_D) has a considerable effect on the internal stability of the RSW. Thus, the number of reinforcement layers (n) can also be obtained for different values of a COV of T_D that ranges from 5% to 10%.
6. The proposed optimum ratio of reinforcement length to wall height (B_2/H_2) ranges from 0.58 and 0.61, and the optimum number of reinforcement layers ranges from 10 to 24. These recommendations are valid when the leachate head (h_w/H_2) increases from 0.2 to 0.8 and the normalized design strength of geosynthetic reinforcement (T_{D_N}) increases from 0.02 to 0.04 when the COV of T_D ranges from 5% to 10% to satisfy the external and internal stability modes simultaneously.

Data Availability Statement

All data, models, and codes generated or used during the study appear in the published article.

Supplemental Materials

Figs. S1–S5, Eqs. (S1)–(S68), and Table S1 are available online in the ASCE Library (www.ascelibrary.org).

References

Annapareddy, V. R., A. Pain, and S. Sarkar. 2017. "Seismic translational failure analysis of MSW landfills using modified pseudo-dynamic approach." *Int. J. Geomech.* 17 (10): 04017086. https://doi.org/10.1061/(ASCE)GM.1943-5622.0000990.

Babu, G. L. S., and B. M. Basha. 2008. "Optimum design of cantilever retaining walls using target reliability approach." *Int. J. Geomech.* 8 (4): 240–252. https://doi.org/10.1061/(ASCE)1532-3641(2008)8:4(240).

Babu, G. L. S., K. R. Reddy, and A. Srivastava. 2014. "Influence of spatially variable geotechnical properties of MSW on stability of landfill slopes." *J. Hazard. Toxic Radioact. Waste* 8 (1): 27–37. https://doi.org/10.1061/(ASCE)HZ.2153-5515.0000177.

Basha, B. M., and P. K. Basudhar. 2010. "Pseudo static seismic stability analysis of reinforced soil structures." *Geotech. Geol. Eng.* 28 (6): 745–762. https://doi.org/10.1007/s10706-010-9336-2.

Basha, B. M., and G. L. Babu. 2011. "Reliability based earthquake resistant design for internal stability of reinforced soil structures." *Geotech. Geol. Eng.* 29 (5): 803–820. https://doi.org/10.1007/s10706-011-9418-9.

Chalermyanont, T., and C. H. Benson. 2004. "Reliability-based design for internal stability of mechanically stabilized earth walls." *J. Geotech. Geoenviron. Eng.* 130 (2): 163–173. https://doi.org/10.1061/(ASCE)1090-0241(2004)130:2(163).

Choudhury, D., and P. Savoikar. 2010. "Seismic stability analysis of expanded MSW landfills using pseudo-static limit equilibrium method." *Waste Manage. Res.* 29 (2): 135–145. https://doi.org/10.1177/0734242X10375333.

Duncan, M. J. 2000. "Factors of safety and reliability in geotechnical engineering." *J. Geotech. Geoenviron. Eng.* 126: 307–316.

Ering, P., and G. L. S. Babu. 2016. "Slope stability and deformation analysis of Bangalore MSW landfills using constitutive model." *Int. J. Geomech.* 16 (4): 04015092. https://doi.org/10.1061/(ASCE)GM.1943-5622.0000587.

FHWA (Federal Highway Administration). 2001. *Mechanically stabilized earth walls and reinforced soil slopes: Design and construction guidelines*. FHWA-NHI-00-43. Washington, DC: Federal Highway Administration and National Highway Institute.

Gao, W., X. C. Bian, W. J. Xu, and Y. M. Chen. 2018. "Storage capacity and slope stability analysis of municipal solid waste landfills." *J. Perform. Constr. Facil.* 32 (4): 04018036. https://doi.org/10.1061/(ASCE)CF.1943-5509.0001180.

Giroud, J. P., J. G. Zornberg, and A. Zhao. 2000. "Hydraulic design of geosynthetic and granular liquid collection layers." *Geosynth. Int.* 7 (4–6): 285–380. https://doi.org/10.1680/gein.7.0176.

Isenberg, R. H. 2003. "Landfill and waste geotechnical stability." In *USEPA Bioreactor Workshop*, 1–29. Arlington, VA: Solid Waste Landfill Publications.

Jafari, N. H., T. D. Stark, and T. Thalhamer. 2017. "Progression of elevated temperatures in municipal solid waste landfills." *J. Geotech. Geoenviron. Eng.* 143 (8): 05017004. https://doi.org/10.1061/(ASCE)GT.1943-5606.0001683.

Jang, Y. S., Y. M. Kim, and S. I. Lee. 2002. "Hydraulic properties and leachate level analysis of Kimpo metropolitan landfill, Korea." *Waste Manage.* 22 (3): 261–267. https://doi.org/10.1016/S0956-053X(01)00019-8.

Khasawneh, Y. A., and Y. Zhang. 2020. "Numerical analysis of a municipal solid waste slope failure." In *Geo-Congress 2020: Engineering, Monitoring, and Management of Geotechnical Infrastructure*, Geotechnical Special Publication 316, edited by J. P. Hambleton, R. Makhnenko, and A. S. Budge. Reston, VA: ASCE.

Kocasoy, G., and K. Curi. 1995. "The Ümraniye-Hekimbashi open dump accident." *Waste Manage. Res.* 13: 305–314.

Koerner, R. M., and T.-Y. Soong. 2002. "Stability assessment of ten large landfill failures." In *Advances in Transportation and Geoenvironmental Systems Using Geosynthetics*, *Geotechnical Special Publication 103*, edited by J. G. Zornberg and B. R. Christopher, 1–38. Reston, VA: ASCE.

Landva, A. O., A. J. Valsangkar, and S. G. Pelkey. 2000. "Lateral earth pressure at rest and compressibility of municipal solid waste." *Can. Geotech. J.* 37 (6): 1157–1165. https://doi.org/10.1139/t00-057.

Ling, H. I., D. Leshchinsky, Y. Mohri, and T. Kawabata. 1998. "Estimation of municipal solid waste landfill settlement." *J. Geotech. Geoenviron. Eng.* 124 (1): 21–28.

Mahapatra, S., B. M. Basha, and B. Manna. 2020. "System reliability framework for design of MSE walls for vertical expansion of MSW landfills." *J. Hazard. Toxic Radioact. Waste* 25 (1): 04020060. https://doi.org/10.1061/(ASCE)HZ.2153-5515.0000559.

McEnroe, B. M. 1993. "Maximum saturated depth over landfill liner." *J. Environ. Eng.* 119 (2): 262–270. https://doi.org/10.1061/(ASCE)0733-9372(1993)119:2(262).

Merry, S. M., E. Kavazanjian, and W. U. Fritz. 2005. "Reconnaissance of the July 10 2000, Payatas landfill failure." *J. Perform. Constr. Facil.* 19: 100–107. https://doi.org/10.1061/(ASCE)0887-3828(2005)19:2(100).

Phoon, K. K., and F. H. Kulhawy, 1999. "Characterization of geotechnical variability." *Can. Geotech. J.* 36 (4): 612–624. https://doi.org/10.1139/t99-038.

Qian, X. 2008. "Limit equilibrium analysis of translational failure of landfills under different leachate buildup conditions." *Water Sci. Eng.* 1 (1): 44–62. https://doi.org/10.1016/S1674-2370(15)30018-1.

Qian, X., D. H. Gray, and R. M. Koerner. 2004. "Estimation of maximum liquid head over landfill barriers." *J. Geotech. Geoenviron. Eng.* 130 (5): 488–497. https://doi.org/10.1061/(ASCE)1090-0241(2004)130:5(488).

Qian, X., and R. M. Koerner. 2007. *Translational failure analysis of solid waste landfills including seismicity and leachate head calculations*. Folsom, CA: Geosynthetic Research Institute.

Raghuram, A. S. S., and B. M. Basha. 2021. "Second-order reliability-based design of unsaturated infinite soil slopes." *Int. J. Geomech.* 21 (4): 04021024. https://doi.org/10.1061/(ASCE)GM.1943-5622.0001954.

Rowe, R. K., and Y. Yu. 2010. "Factors affecting the clogging of leachate collection systems in MSW landfills." In Vol. 1 of *Proc., 6th Int. Congress on Environmental Geotechnics*, 3–23. London: International Society for Soil Mechanics and Geotechnical Engineering (ISSMGE).

Savoikar, P., and D. Choudhury. 2012. "Translational seismic failure analysis of MSW landfills using pseudodynamic approach." *Int. J. Geomech.* 12 (2): 136–146. https://doi.org/10.1061/(ASCE)GM.1943-5622.0000127.

Sheng, H., Y. Ren, M. Huang, Z. Zhang, and J. Lan. 2021. "Vertical expansion stability of an existing landfill: A case study of a landfill in Xi'an, China." *Adv. Civ. Eng.* 2021: 5574238. https://doi.org/10.1155/2021/5574238.

Sia, A. H. I., and N. Dixon. 2007. "Distribution and variability of interface shear strength and derived parameters." *Geotext. Geomembr.* 25 (3): 139–154. https://doi.org/10.1016/j.geotexmem.2006.12.003.

Singh, M. K., J. S. Sharma, and I. R. Fleming. 2009. "Shear strength testing of intact and recompacted samples of municipal solid waste."*Can. Geotech. J.* 46 (10): 1133–1145. https://doi.org/10.1139/T09-052.

Yang, R., Z. Xu, and J. Chai. 2019. "Seepage analysis of a multilayer waste slope considering the spatial and temporal domains of permeability." *Adv. Civ. Eng.* 2019: 3689097. https://doi.org/10.1155/2019/3689097.

Yang, R., Z. Xu, and J. Chai. 2020. "Numerical analysis of three-dimensional infiltration in a municipal solid waste landfill under rainfall." *Pol. J. Environ. Stud.* 29 (2): 1953–1963. https://doi.org/10.15244/pjoes/110044.

Young-Seok, J., Y. Wan-Kyu, H. Sung-Phil, and K. Chang-Yong. 2022. "Coupled mechanical creep and bio-compression and residual settlement in a multi-stage municipal solid waste landfill, Korea." *Sci. Rep.* 12 (1): 1–9.

Zhan, T. L. T., X. B. Xu, M. C. Yun, X. F. Ma, and J. W. Lan. 2015. "Dependence of gas collection efficiency on leachate level at wet municipal solid waste landfills and its improvement methods in China." *J. Geotech. Geoenviron. Eng.* 141 (4): 04015002. https://doi.org/10.1061/(ASCE)GT.1943-5606.0001271.

Zhang, Y., X. L. Feng, and T. Liu. 2013. "Study on earth pressure and engineering properties of solid waste during foundation pit excavation." *Appl. Mech. Mater.* 353: 790–794. https://doi.org/10.4028/www.scientific.net/AMM.353-356.790.

Zhang, Z., Y. Wang, Y. Fang, X. Pan, J. Zhang, and H. Xu. 2020. "Global study on slope instability modes based on 62 municipal solid waste landfills." *Waste Manage. Res.* 38 (12): 1389–1404. https://doi.org/10.1177/0734242X20953486.